• U C •

FCTUC FACULDADE DE CIÊNCIAS
E TECNOLOGIA
UNIVERSIDADE DE COIMBRA

DEPARTAMENTO DE
ENGENHARIA MECÂNICA

Assessment of measuring techniques to study the deflection of a ceramic tile during ballistic impact

Dissertação apresentada para a obtenção do grau de Mestre em Engenharia Mecânica na Especialidade de Energia e Ambiente

Autor

Peter Daniel Gonçalves Santos

Orientadores

Professor Doutor José Manuel Baranda Ribeiro

Professora Doutora Cristina Maria Gonçalves dos Santos Louro

Juri

Presidente	**Professora Doutora Ana Paula Bettencourt Martins Amaro**
	Professora Auxiliar da Universidade de Coimbra
Vogal	**Professora Doutora Maria Augusta Neto**
	Professora Auxiliar da Universidade de Coimbra
Orientador	**Professor Doutor José Manuel Baradna Ribeiro**
	Professor Auxiliar da Universidade de Coimbra

Colaboração Institucional

TNO innovation for life **TNO Innovation for life**

Coimbra, Fevereiro, 2014

“I am prepared for the worst but hope for the best”

Benjamin Disraeli

To my parents

ACKNOWLEDGMENT

The following Master Thesis could not have been possible without the contribution of several people that I am proud to mention here.

I would like to express the deepest appreciation to my committee chair Professors Cristina Louro and José Baranda for giving me the courage and advice necessary to accomplish a successful Master Thesis.

To my traineeship mentor Dr. Erik Carton as well as all staff of TNO for the generosity and knowledge they gave me, asking only for hard work in exchange.

To all the teachers in DEM. Although they did not help directly on this report, they gave me a sense of responsibility and adaptability that was present during all my traineeship experience.

To my friends who shared my magical academic experience. I will have you in mind during every important moment of my life.

To Daianna León for the moral support and comprehension always present in her daily speech.

To my brothers, for giving me the sense of hard work in order to achieve success, as well as holding my head up when life does not go as expected.

And last but not least, to my parents. I will always treasure your dedication and love that made me the person I am today.

ABSTRACT

Earlier work on ceramic armor has focused on the cracking behaviour of bare tiles upon projectile impact. Some of the earliest cracks are radial cracks which are formed on the back of the tiles due to tensile stresses that occur by consequence of local bending of the tile.

This research focusses on studying the deflection of a ceramic tile during ballistic impact. The detail screening of the potential available techniques for the study of such phenomena, characterized by microsecond temporal and micrometer spatial scales, extremely difficult to achieve together, is one of the objectives of this research work.

The deflection measuring techniques to be studied are divided in two groups; Optical and Electrical. The physical principles behind each one of these groups and their advantages and disadvantages, taking into account aspects such as accuracy, facility of assessment and cost will be detailed described.

Keywords Deflection, Ballistic, Ceramic tile, Alumina, Silicon carbide, Measuring techniques.

RESUMO

Um dos aspectos mais importantes, e dos mais estudados, do comportamento balístico – ao impacto de alta velocidade – de materiais cerâmicos é o que diz respeito ao mecanismo de fractura. Sabe-se que a fractura destes materiais, nestas situações, ocorre sob a forma radial, na face oposta à do impacto, devido à formação de tensões de tração como resultado da deflexão localizada.

Este trabalho está focado no estudo da deflexão de alvos cerâmicos durante o impacto balístico. O levantamento das técnicas potencialmente disponíveis para a caracterização experimental deste fenómeno, que envolve tempo característicos da ordem dos microssegundos e resoluções espaciais da ordem dos micrómetros, cujo alcance combinado é extremamente exigente, será um dos objectivos principais deste trabalho.

As técnicas de caracterização estudadas foram divididas em dois grandes grupos: as ópticas e as eléctricas. Os princípios físicos por de trás de cada um destes grupos são apresentados e são ainda discutidas as principais vantagens e desvantagens tendo em conta a precisão a facilidade de implementação e o custo de cada uma dessas técnicas.

Palavras chave Deflexão, Balística, Alvo cerâmico, Alumina, Carboneto de silício, Técnicas de medida.

Index

Figure index v

Table index viii

Simbology ix
Simbols ix
Acronyms x

1. Introduction 1

2. Pre-studies on ceramic tile deflection 2

3. Measuring techniques 7
3.1. Optical Methods 7
3.1.1. Digital Image Correlation and High speed camera 7
3.1.2. Deflectometry 8
3.1.3. Newton rings 10
3.1.4. Moiré Fringes 12
3.1.5. Shadowmetry 15
3.2. Electrical methods 17
3.2.1. Capacitive displacement sensors 18
3.2.2. Eddy current displacement sensors 19

4. Results and Discussions 22
4.1. Static Deflectometry experiments 22
4.1.1. Brass material results 24
4.1.2. SiC material results 28
4.1.3. Al_2O_3 material results 32
4.2. Dynamic Deflectometry Experiments 38
4.2.1. Al_2O_3 material results 40
4.2.2. SiC material results 44

5. Conclusions 50

References 52

Websites 53

FIGURE INDEX

Figure 1- Schematic illustration of ballistic impact on a ceramic tile 2

Figure 2- The bending of a 10mm Alumina tile during the first 5μs, from red to orange, the time increases from 1 to 5 μs (Ditzhuijzen C.S.E, October 2013) 3

Figure 3-Composed beam theory relation between plate thickness and displacement until fracture (600MPa) tensile stress (Frade J. 2012). 4

Figure 4-Finite element relation between plate thickness t and displacement δ until fracture (600MPa) (Frade J. 2012) 5

Figure 5-The sequence of observed damage effects for Alotec tiles after impact of a .30 AP M2 bullet (Ditzhuijzen C.S.E., et.al., August 2013). 5

Figure 6- Image sequence of an impact on a Al2O3 tile from a 7.62 APM2 bullet at a velocity of 830 m/s (Carton E.P., 2012) 6

Figure 7-DIC and high speed camera setup 8

Figure 8- Experimental setup of the Deflectometry experiment 9

Figure 9- Convex tile image reflection used in Deflectometry method 9

Figure 10- Trigonometric approach used in Deflectometry method 10

Figure 11- Origination of Newton Rings 11

Figure 12- Newton rings on the ballistic tile 11

Figure 13- Moiré Fringe experience used in this study 13

Figure 14-Comparison between reference surface (left) deformed surface (right), obtained by Moiré Fringes measuring technique. 13

Figure 15- Experimental setup of Moiré Fringe employed in this study 14

Figure 16- Shadowmetry technique setup scheme operated in this study 16

Figure 17- illustration model for calculations of the shadow size crated by an object obstruction 16

Figure 18- Capacitor displacement sensor 19

Figure 19- Eddy current Displacement sensor 20

Figure 20- Precision Dial Gauge applied to a brass plate 22

Figure 21- Optical experiment for deflectometry 23

Figure 22-Example of a reflected image deformation of the brass plate 24

Figure 23-Graphic result analyses of deflectometry on a mechanically measured 0.12mm dent size on a brass plate 25

Figure 24-Graphic result analyses of deflectometry on a mechanically measured 0.42mm dent size on a brass plate 26

Figure 25-Experimental Deflection measurement on a brass plate 26
Figure 26-SiC reflective surface with (left) and without (right) polymer coating 28
Figure 27-Experimental setup of the position of the components necessary for the Deflectometry experiment 29
Figure 28-Deflection measurement on the SiC ceramic tile 30
Figure 29- Analyses of the influence of the position of the grid and camera on the measurement results 32
Figure 30- Reflective properties of the coating on Al_2O_3 (right) and SiC (left) tiles 33
Figure 31- Experimental setup using high speed video 34
Figure 32- Al_2O_3 and SiC reflective surface obtained with Shimadzu high speed camera and 300mm lens 34
Figure 33- SiC tile Shimadzu image of a 0.56mm dent 35
Figure 34- Deflection measurement on a ceramic tile Al_2O_3 36
Figure 35- Real and program assumed SiC dent shape. 37
Figure 36-Side view (left) and Isometric view (right) of the experimental setup for the deflectometry experiment during ballistic impact 38
Figure 37- Side view of the deflection shape on a Al_2O_3 tile (7mm) during ballistic impact of a 7.62 APM2 bullet with a velocity of 830m/s at a time of 14μs after impact (Carton E.P. and Roibrocks R., 2012) 39
Figure 38- Different frames from projected lines on an Al_2O_3 tile during ballistic impact by a 7.62 APM2 bullet 40
Figure 39- Image of a Al_2O_3 tile during ballistic impact by a 7.62 APM2 bullet using deflectometry method to measure the dent size x at 11μs 41
Figure 40- Relation between dent size (x) and time after impact of a 7mm Al_2O_3 tile during ballistic impact by a 7.62 APM2 bullet 43
Figure 41- Relation between time after impact and deformation velocity of a 7mm Al_2O_3 tile during ballistic impact by a 7.62 APM2 bullet 43
Figure 42- Different frames from projected lines on an SiC tile during ballistic impact by a 7.62 APM2 bullet 44
Figure 43- Image of a SiC tile during ballistic impact by a 7.62 APM2 bullet using deflectometry method to measure the dent size x 11μs after the first deformation of the tile's rear surface 45
Figure 44- Relation between dent size (x) and time after impact of a SiC tile during ballistic impact by a 7.62 APM2 bullet 46
Figure 45- Relation between time after impact and the deformation velocity of a SiC tile during ballistic impact by a 7.62 APM2 bullet 46
Figure 46-Different frames from projected lines on an SiC tile during ballistic impact by a 7.62 APM2 bullet 47

Figure 47- Relation between dent size (x) and time after impact of a SiC tile during ballistic impact by a 7.62 APM2 bullet 48

Figure 48- Relation between time after impact and the deformation velocity of a SiC tile during ballistic impact by a 7.62 APM2 bullet 48

TABLE INDEX

Table 1-Crack appearances for radial and conical for alumina tiles hit by 7.62 APm2 ball at 830 m/s (Ditzhuijzen C.S.E, October 2013) 3

Table 2- Pros and cons of each technique 21

Table 3- Dial Gauge measurement of maximal height of dents in brass plates 23

Table 4- Optical measurements using deflectometry method of a mechanically measured 0.12 mm dent size on a brass plate 25

Table 5- Optical measurements using deflectometry method of a mechanically measured 0,42 mm dent size on a brass plate 25

Table 6- Mechanical and Optical Measurement of a brass plate 27

Table 7- Mechanical and Optical Measurement of a dent on a ceramic SiC tile 29

Table 8- Mechanical and Optical Measurement of a dent on a ceramic SiC tile 30

Table 9- Mechanical and Optical Measurement of a dent on a ceramic tile using a Grid with 8mm lines 31

Table 10- Image ,I, Object ,o, and dent width , Ø, influence on Deflectometry measuring technique 31

Table 11- Results of the influence of the position of the camera and grid during measurements 32

Table 12- Mechanical and Optical Measurement of a 0.54mm dent on a SiC tile using a Shimadzu high speed camera and a Grid with 4mm lines 35

Table 13- Mechanical and Optical Measurement of a dent on a ceramic Al_2O_3 tile using a grid with 2mm width of grid lines 36

Table 14- Dent calculation Excel sheet for a 7mm thick Al_2O_3 tile during ballistic impact by a 7.62 APM2 bullet using deflectometry method 42

Table 15- Relation between dent size (x) and deformation velocity of a 7mm Al_2O_3 tile during ballistic impact by a 7.62 APM2 bullet 43

Table 16- Dent calculation Excel sheet for a 8mm thick SiC tile during ballistic impact by a 7.62 APM2 bullet using deflectometry method 45

Table 17- Dent size (x) and deformation velocity for 3 to 13µs during ballistic impact by a 7.62 APM2 bullet 47

Table 18- Dent size (x) and deformation velocity for 3 to 11µs during ballistic impact by a 7.62 APM2 bullet 49

SIMBOLOGY

Simbols

$\boldsymbol{A}$ − Area of plates

$\boldsymbol{a}$ − Distance of the object to the screen

$\boldsymbol{b}$ − Length of the light source

$\boldsymbol{C}$ − Capacitance

$\boldsymbol{d_o}$ − Distance between real image and convex surface

$\boldsymbol{d_I}$ − Distance between virtual image and convex surface

$\boldsymbol{d_1}$ − Distance from screen to light source

$\boldsymbol{d_2}$ − Distance between plates

$\boldsymbol{f}$ − Focal point

$\boldsymbol{f}$ − Frequency

$\boldsymbol{g}$ − Distance between lines on the grid

$\boldsymbol{I}$ − Width of virtual image

$\boldsymbol{k}$ − Dielectric constant of material between plates

$\boldsymbol{M}$ − Magnification

$\boldsymbol{m}$ − Number of bright lines

$\boldsymbol{M_\theta}$ − Bending moment of circumferential surface

$\boldsymbol{M_r}$ − Bending moment on radial plane

$\boldsymbol{M_2}$ − Mass of projectile

$\boldsymbol{n}$ − Number of lines of virtual image

$\boldsymbol{N_r}$ − In-plane radial force intensity

$\boldsymbol{O}$ − Dimension of the object

$\boldsymbol{o}$ − Width of real image

$\boldsymbol{p}$ − Pitch of Moiré Fringe

$\boldsymbol{t_1}$ − Thickness of the air film between lens

$\boldsymbol{R}$ − Radius of curvature of the mirror

$\boldsymbol{r}$ − Radius of the Newton Ring

$\boldsymbol{r_m}$ – Radius of projectile

$\boldsymbol{S}$ – Size of the shadow

$\boldsymbol{t}$ – Time

$\boldsymbol{W}$ – Transverse displacement

$\boldsymbol{x}$ – Deflection of the tile / dent size

$\boldsymbol{X_0}$ – Object surface

$\boldsymbol{X_r}$ – Fringe position

$\boldsymbol{Y}$ – Yield stress

$\boldsymbol{Z}$ – Surface deviation

$\boldsymbol{\lambda}$ – Wave length of light

$\boldsymbol{\rho}$ –Density

$\boldsymbol{\epsilon_0}$ – Permeability of free space constant

$\boldsymbol{\delta}$ – Penetration depth

$\boldsymbol{\mu}$ – Mmagnetic permeability

$\boldsymbol{\sigma}$ – Electric conductivity

∅ – Dent diameter of the convex surface

$\boldsymbol{\theta_1}$ – Angle of incidence of light

$\boldsymbol{\theta_2}$ – View angle

Acronyms

DEM – Departamento de Engenharia Mecânica

FCTUC – Faculdade de Ciências e Tecnologia da Universidade de Coimbra

TNO – The Netherlands Organization, Innovation for life

1. INTRODUCTION

Studying the behaviour of ceramics is crucial for armor materials. They have been used for their unique properties such as hardness and light weight, matters of extreme importance during ballistic impact situations. In order to manage these properties and sometimes manipulate them, it is important to understand every moment of reaction to a ballistic impact. Therefore, it is imperative to study every microsecond of a bullet impact.

The present dissertation was elaborated with the collaboration of TNO-Innovation for life. Being a company with vast knowledge in ballistics and explosions, it was easy to choose this company to work at. In order to absorve as much information and experience as possible, a three month traineeship was performed at the company in Delft, Holland. The experimental part of the work was developed at TNO in Holland, at the ballistic Laboratory.

When arrived to TNO, I was proposed to create/find a measuring technique, capable of measuring small deflections (μm) in short periods of time (μs). This task had not been yet studied experimentally what turned it even more interesting both for me and TNO that is a scientific community with focus on various themes. The main subjects of the company are Industrial innovation, Healthy living, Energy, Mobility, Built environment, Information society and Defence, Safety and Security, being the last one, the department where my work was performed.

This dissertation is divided in five main Chapters.

In Chapter 2, a brief resume is presented concerning previous studies on this subject.

Chapter 3 is dedicated to the working methodologies and describes the measurement procedures as the measuring techniques.

The results of this study and the respective discussion are made in Chapter 4.

The last chapter is a final overview of all measuring techniques studied, observations and advices for future investigations on this matter.

2. PRE-STUDIES ON CERAMIC TILE DEFLECTION

TNO provided several studies of ballistic impact on ceramic tiles. Their organization and knowledge on ballistic matters was a huge support for this work. The following studies show various reports performed by TNO where important information was analysed in order to have the best performance as possible on this matter.

A schematic illustration of the ballistic impact on a ceramic tile is shown in Figure 1. As can be seen, the bullet impact will create a deflection on the tiles rear surface approximately 2μs after impact. This deflection will be uniform before the appearance of any crack and shattered after the cracking begins. It seems that this behavior occurs in very short times, near 20μs. It is important to notice that this deformation occurs in the plastic domain. This will be a behavior to be studied on this work for the first time ever in the world.

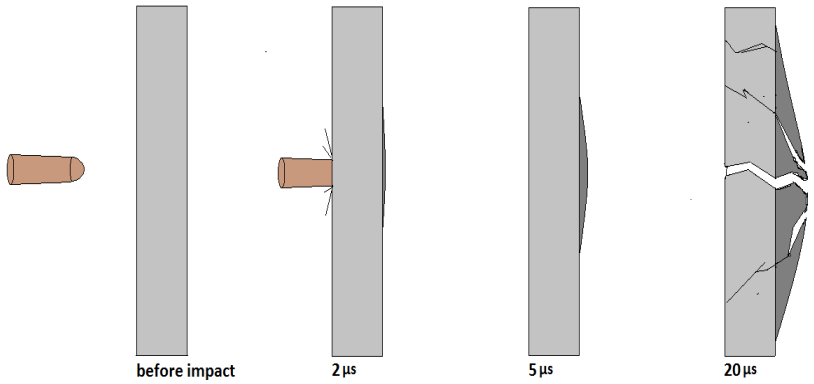

Figure 1- Schematic illustration of ballistic impact on a ceramic tile

In order to begin this study, TNO reports on tile deflection (Ditzhuijzen C.S.E, et al, August 2013) and crack detection in armor plates (Ditzhuijzen C.S.E, October 2013) have been studied.

These reports provided the instant of cracks appearing and therefore to know what timeframe to study elastic deflection until fracture. Table 1, elaborated by Ditzhuijzen C.S.E (August 2013), provides the moments of radial and conical crack appearance for alumina tiles (Alotec 98 is the commercial name) upon impact of a projectile bullet. It shows that at impact velocities between 810 m/s and 850 m/s and tiles thickness between 6

and 15mm, radial cracking occurs between 2 and 7 microseconds after impact. It is possible to understand that for larger thicknesses, latter the cracks will appear. From radial cracks appearing at 3μs for 6mm thicknesses, until radial crack appearance at 7μs for tile thicknesses of 12mm.

Table 1-Crack appearances for radial and conical for alumina tiles hit by 7.62 APm2 ball at 830 m/s (Ditzhuijzen C.S.E, October 2013)

Impact velocity (m/s)	Material	Thickness (mm)	Projectile	Start Rad (μs)	Conical (μs)
834	Alotec 98	10	.30 AP M2	*4*	*17*
837	Alotec 98	10	.30 AP M2	*4*	*12*
834	Alotec 98	12	.30 AP M2	*7*	*9*
842	Alotec 98	12	.30 AP M2	*7*	*19*
831	Alotec 98	15	.30 AP M2	*4*	*7*
838	Alotec 98	15	.30 AP M2	*5*	*16*
852	Alotec 98	8	.30 AP M2	4	6
842	Alotec 98	8	.30 AP M2	6	8
857	Alotec 98	6	.30 AP M2	2	4
817	Alotec 98	6	.30 AP M2	3	3
842	Alotec 98	6	.30 AP M2	3	4
825	Alotec 98	6	7.62 Ball (Sintox)	*3*	*4*

In another work, Ditzhuijzen C.S.E (October 2013) made a macroscopic dynamic model of tile deflection by using Euler Bernoulli beam theory. The results obtained by using the Wolfram Mathematica 7.0, are presented in Figure 2 for 10mm alumina tiles. The analyses of the evolution allows to understand the deflection during the first periods of time after impact. It shows that for 10mm alumina tiles during ballistic impact, the displacement of the rear of the impact zone will increase from 2μm for the 1μs, until 14μm correspondent to 5μs after impact.

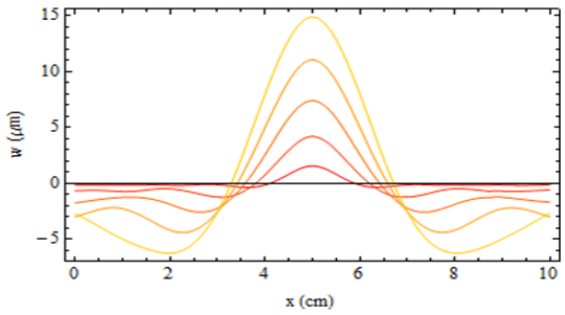

Figure 2- The bending of a 10mm Alumina tile during the first 5μs, from red to orange, the time increases from 1 to 5 μs (Ditzhuijzen C.S.E, October 2013)

Other important studies concerning material deformation during ballistic impact have been studied. Shock and ballistic properties of bainitic steel and tungsten alloys were performed by Hammond R (2004). This work gave us an overview on determination of penetration and perforation properties, determination of static properties, stress and strain measurements, high speed photography, microstructural studies, shock properties of bainitic steels and impact on free plates. In Field J. E., et al. (2004), an overview of experimental techniques for shock and high rate deformation are studied. The focus in this report is on optical techniques for dynamic stress analysis. The mentioned techniques were Moiré, laser speckle and interferometry.

The report on simulation of ballistic impact on armored civil vehicles made by Adams B. (2003), that had the contribution of TNO with high strain rate measurement and impact projectiles, vised to clarify aspects of measurement of the penetration depth and crater radius, x-ray system to measure the nose and tail position at different times during penetration and high-speed imaging.

Another student from DEM-UC, that did a traineeship at TNO in 2012, Frade J. (2012) also elaborated two different ways to calculate deflection by bending of a ceramic tile with Al backing. He used the composed beam theory, giving an analytical approach to the study, and finite element analyses using Autodesk Inventor Professional 2012. Figure 3 and 4 show some relevant results by the analytical composed beam theory elaborated by Frade J. (2012). Analysing Figure 3 we can understand the evolution of the displacement according to the tiles thickness, using composed beam theory, it is clear that larger thicknesses correspond to smaller displacements.

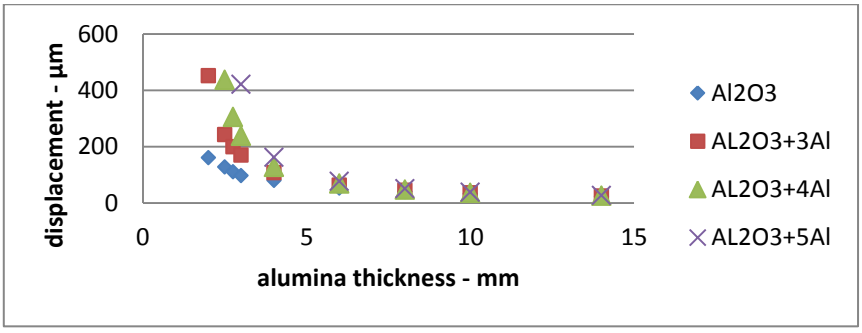

Figure 3-Composed beam theory relation between plate thickness and displacement until fracture (600MPa) tensile stress (Frade J. 2012).

Analyzing Figure 4, the results are similar to those of, that are, Figure 3, although using finite element relations between thickness and displacement show smaller displacements.

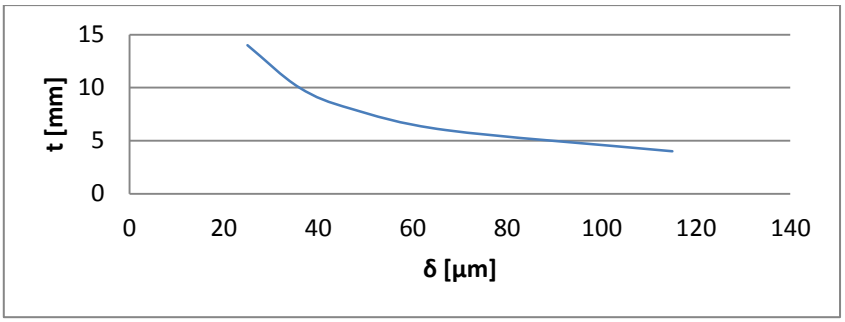

Figure 4-Finite element relation between plate thickness t and displacement δ until fracture (600MPa) (Frade J. 2012)

Figure 5 shows the damage sequence of a ceramic tile during ballistic impact obtained by Ditzhuijzen C.S.E., (August 2013). Radial cracks are the first to appear, independently of the tile thickness, followed by concentric cracks.

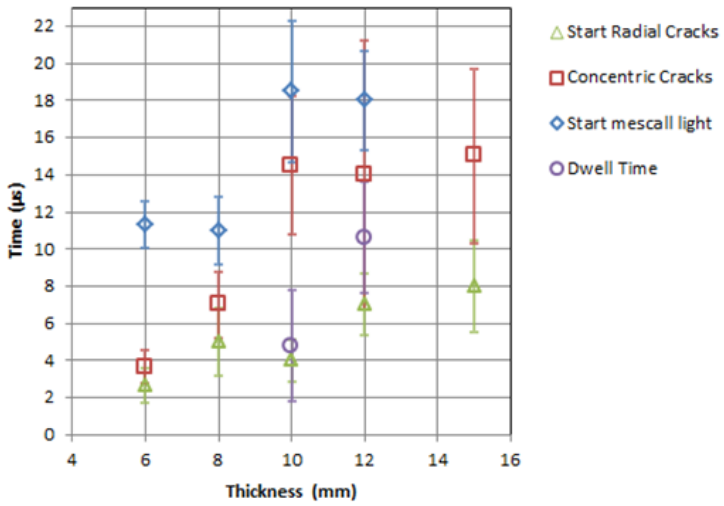

Figure 5-The sequence of observed damage effects for Alotec tiles after impact of a .30 AP M2 bullet (Ditzhuijzen C.S.E., et.al., August 2013).

According to the study developed in alumina ceramics by Carton, E.P. (2012), it is showed in Figure 6 a sequence of images from an impact of a 7.62 APM2 bullet with a velocity of 830 ±10 m/s on a 100×100×7 mm Al2O3 tile. It is important to know the size of the dent provoked by the projectile during different moments after impact. We can

notice that this deflection is only perceptible 8μs after impact and possible to be measured 12μs latter. In the image referent to 16μs it is possible to see the tile has been destroyed and a cloud of blast is visible from that moment forward.

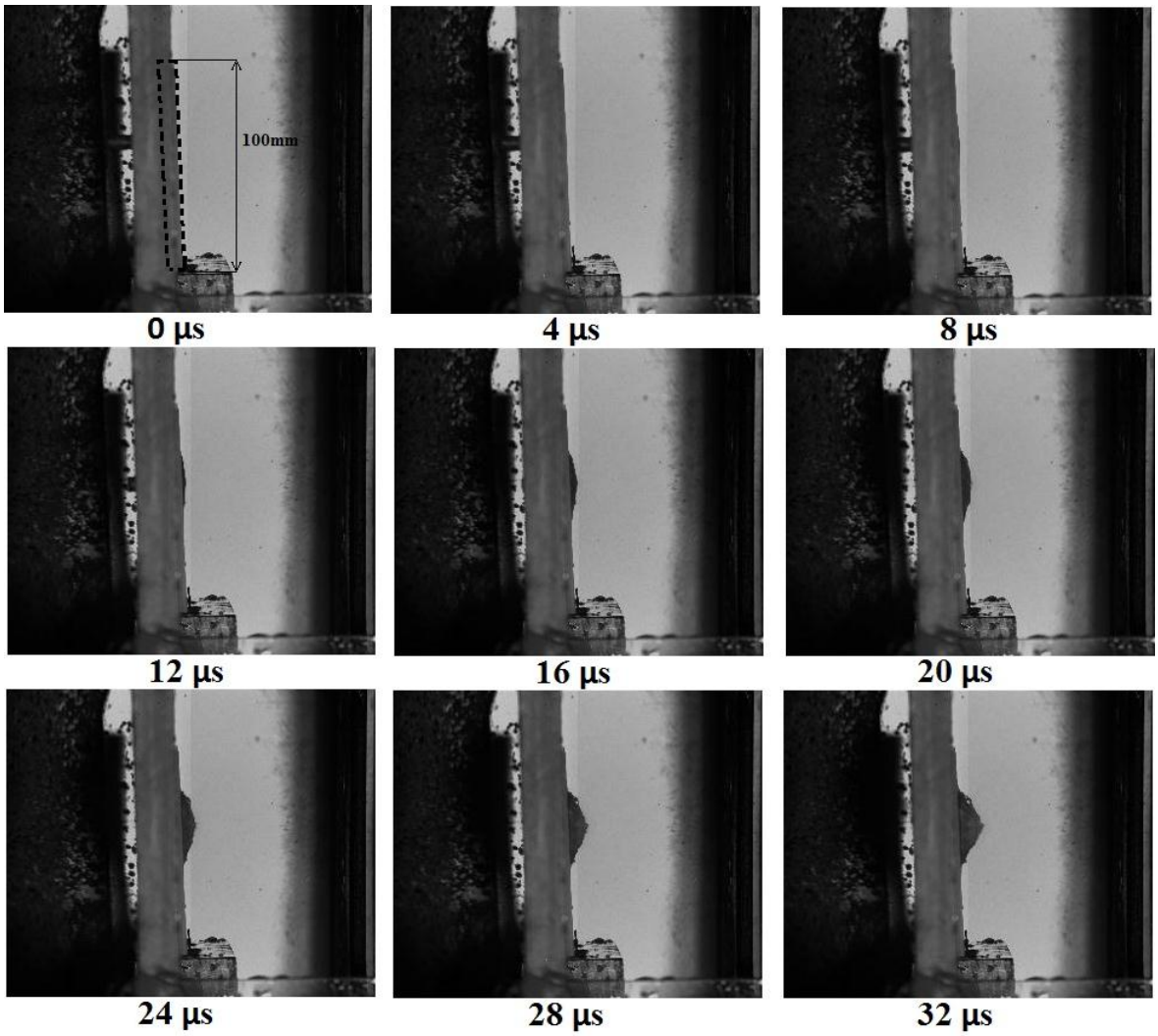

Figure 6- Image sequence of an impact on a Al2O3 tile from a 7.62 APM2 bullet at a velocity of 830 m/s (Carton E.P., 2012)

3. MEASURING TECHNIQUES

In order to fulfil the objectives of this study and based on previous work on this field, both optical and electrical methods must be overviewed.

3.1. Optical Methods

The optical methods assessed in this dissertation were:

- Digital Image Correlation and High speed video;
- Deflectometry;
- Newton rings;
- Moiré fringes;
- Shadowmetry.

3.1.1. Digital Image Correlation and High speed camera

Digital Image Correlation (DIC) is basically a scan of a deformed sample that will then be compared with the sample not deformed. It will compare the equal points between the reference image and the deformed one. The images will be captured by a high definition camera and then processed with algorithmic correlations in order to study all deformations (Bornet M., et al., 2008).

To obtain a precise DIC, it is of extreme importance to define all parameters that will be useful for the input. The more parameters that are in the input, the better results we obtain comparing both model sample and deformed sample. Some of the parameters to set on the input are, namely, pitch or subset overlap, speckle size and density, grey level and interpolation.

Finally the MOIRE software processes the information and evaluates the average grey scale intensity over the subset of both deformed and model sample image to compare them.

In this work, all tiles were prepared with the same dimensions. Nerveless the surfaces were not flat enough to be able to determine such small deformations with

precision up to 10 micrometres (Proulx T., 2013). A DIC scan during a ballistic impact involves perfect imaging of 1000000 images per second time resolution, modelling using hydrocodes (Pretice H.J., et al., 2011) and a controlled environment around all assessment so that no impurities influence the results. Using this method, it is necessary to see two images of the deforming spickeled surface, therefore, it is always necessary either two cameras or one camera plus one mirror. Figure 7 represents the setup for this measuring methology.

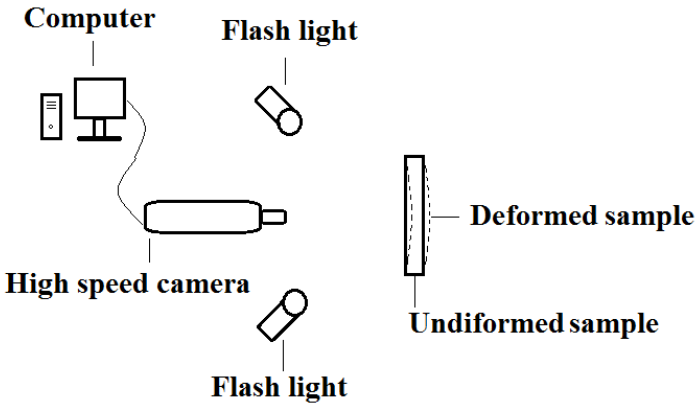

Figure 7-DIC and high speed camera setup

3.1.2. Deflectometry

Deflectometry is a simple non-interferometric method to study small deflections or deformations in any kind of material (Devivier C., et al., 2013). This method allows to study the reflection of surfaces and therefor, their imperfections. Straight lines are projected on the surface to be studied and by the out-of-surface deformation of those lines, the lines are locally curved. The slopes provoked by any deformation can be differentiated so that a curvature analyses can give us any geometrical characterization. The accuracy of this method can be until 3 microns (Surrel Y., 2009).

This method assumes a spherical dent. If the dent deviates from this shape, the results will not be accurate.

For our purpose, this technique seems simple, and easy to apply. If the surface of our tile is made reflective, we can use this technique to measure the deflection assuming that the curved surface works as a convex mirror. The experimental setup in this study is presented in Figure 8. As can be seen, the deflectometry experiment is in the left side and the image obtained when an imperfection is present in the right side. This technique can only be used on perfectly spherical surfaces.

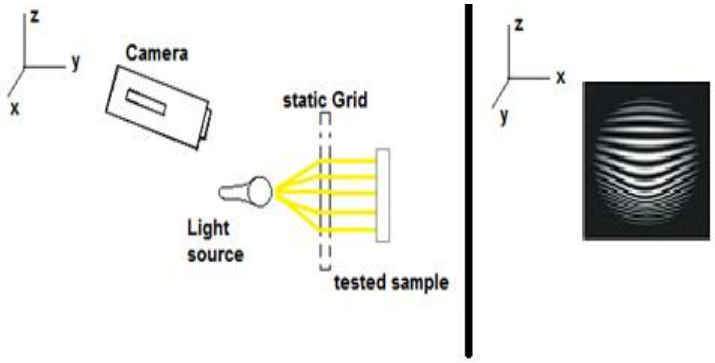

Figure 8- Experimental setup of the Deflectometry experiment

Figure 9 gives a perception of how all calculations are made in order to obtain the deformations dimensions, using a convex mirror as example.

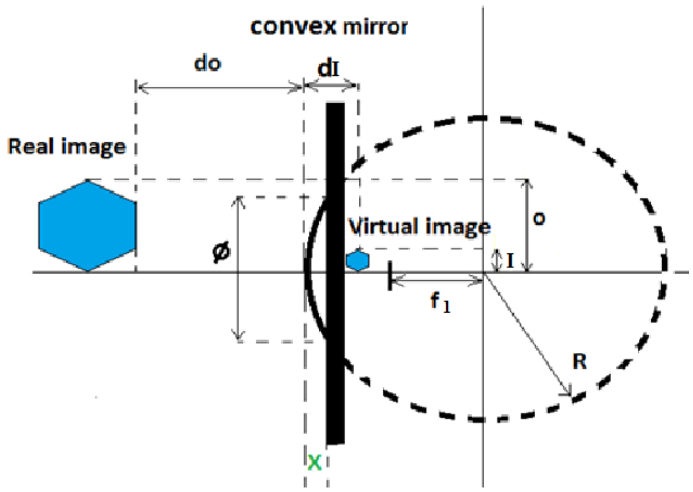

Where:

o-	Width of real image;
I-	Width of virtual image;
R-	Radius of curvature of the mirror;
f_1-	Focal point;
d_0-	Distance between real image and convex mirror;
d_I-	Distance between virtual image and convex mirror;
Ø-	Dent diameter of the convex surface on the tile;
x-	Deflection of the tile.

Figure 9- Convex tile image reflection used in Deflectometry method

The Magnification factor, M, is given by equation (3.1). The relation between the real size of the object ,o, the virtual size of the object, I, and the distance of the object, d_o, will allow to obtain the virtual distance, d_I, .

$$M = \frac{I}{o} = \frac{d_I}{d_o} \tag{3.1}$$

Once we have the virtual distance, d_I, we can use the mirror equation (3.2).The focal point, f, could be achieved by using this equation proposed by Nagata T., et al. (2013).

$$\frac{1}{\mathrm{f}} = \frac{1}{\mathrm{d_o}} + \frac{1}{\mathrm{d_I}} \tag{3.2}$$

Once the focal point, f, is calculated, curvature radius, R, of the mirror could be obtained, having in consideration that a reflection of the surfaces to be analyzed have only one side and therefore, it should be treated as a thin lens with only one surface (Feyman R. 1963);

$$R = 2f \tag{3.3}$$

After having the curvature radius, it is all a matter of trigonometry to find our deflection of the tile x. Figure 10 is an illustration of basic trigonometry used allowing us to find :

$$x = R - \sqrt{\left(R^2 - \frac{\emptyset^2}{2}\right)} \tag{3.4}$$

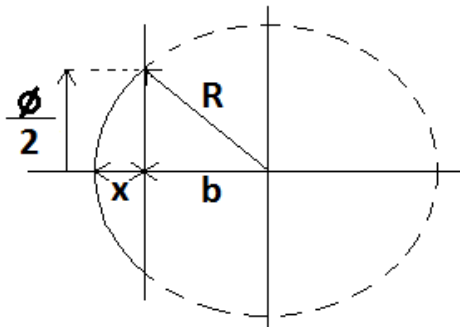

Figure 10- Trigonometric approach used in Deflectometry method

3.1.3. Newton rings

Newton rings are basically visual interferences caused by light that is reflected by an air gap between two surfaces. This reflection gives origin to a series of rings that can be used for various purposes.

When a convex surface is placed on a plane glass sheet, an air film of gradually increasing thickness outward is formed between the lens and the sheet. Therefore, the air gap at the contact point will be zero. If monochromatic light is allowed to fall normally on the convex surface, and the film is viewed in reflected light, alternate bright and dark concentric rings are seen around the point of contact.

Newton Rings can be explained on the basis of wave theory of light. An air film of varying thickness is formed between the curved surface and the glass sheet. When the incident beam of light hits the surface, it will be reflected as well as refracted (Figure

11). When the refracted beam of light hits the glass sheet, we can see a 180º phase change on the reflection. Then, the rings appear between both waves constructively and destructively, provoking light and dark rings (Umesh K. S., et al., 2012).

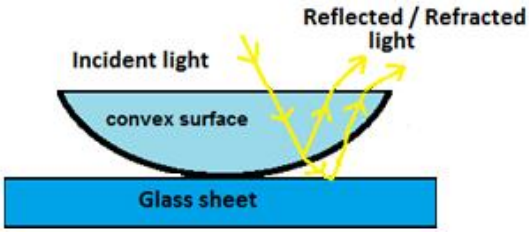

Figure 11- Origination of Newton Rings

For this work, using the ceramic tile as the curved surface, we will study the possibility of measuring the gap of air between the glass plate and the deflected ceramic tile and therefore, the tile deflection during ballistic impact as exemplified on Figure 12.

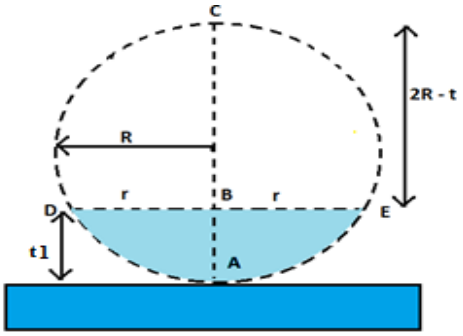

Where:
r- Radius of the ring;
R- Radius of the curvature of the lens;
t_1- Thickness of the air film between the lens and the plate.

Figure 12- Newton rings on the ballistic tile

Thus, following Figure 12, it can be said that:

$$\overline{BD} \times \overline{BE} = \overline{AB} \times \overline{BC}$$
$$r \times r = t(2R - t)$$
$$r^2 = (2Rt - t^2)$$

Once that **t** is infinitely small compared to **r,** we eliminate $\mathbf{t^2}$, and finish with:

$$r^2 = 2Rt \tag{3.5}$$

Considering thin films, path difference $\boldsymbol{\Delta}$ of constructive and destructive interference is given by (Arbor Scientific, 2009). Thus,

- For constructive path:

$$\Delta = m\lambda, with\ m = 1,2,3 \tag{3.6}$$

- For destructive path:

$$\Delta = \frac{m\lambda}{2}, with\ m = 1,2,3, \ldots \tag{3.7}$$

Where:

Δ – Path difference

m – Number of bright rings, being the center ring = 0 and for the Nth ring , $m = N - 1$

λ – Wave length of light

- Finally we obtain the expression for the radius of Nth bright ring:

$$r_n = \sqrt{R\lambda\ (N-1)} \tag{3.8}$$

Where:

$\mathbf{r_n}$ – Radius of the Nth bright ring

And the calculation for the air thickness that will give us the convex lens curvature **t:**

$$t = \frac{\Delta}{2} - \frac{\lambda}{4} \tag{3.9}$$

3.1.4. Moiré Fringes

Moiré patterns are images produced when an observer looks through two or more grids. They are used to study interferometric results. By superposing two grids that are composed of parallel lines slightly displaced relative to the other, Moiré fringes are produced (Creath K. and Wyant J. C., 1992).

Basically, a non-contact grid is created parallel to the object. This grid is called reference grating. Another grid is fixed to the object to be deformed or moved and is called specimen grating.

The next example will serve to explain how this technique could work in order to achieve our goal.

This experiment would we composed by a projected grid on the object surface at an angle of θ_0. When the object surface suffers any kind of deformation, a projected grating line will be displaced at the distance Δu and captured on camera.

Mathematically, the relation between Δu and the surface deviation ΔZ will be given by (Creath K. and Wyant J. C., 1992), that is:

$$Z = \frac{x_0 - x_R}{tan\,\theta_0} = \frac{\Delta u}{tan\,\theta_0} = \frac{m_p}{sin\theta_0} \quad (3.10)$$

Where:

x_R- Fringe positions on the reference and object surface respectively;

x_0- Fringe position on the object surface;

m_p - Magnification of the projection.

Figure 13 shows the positioning of the projector in relation with the camera, as well as the object surface superimposed on the reference surface.

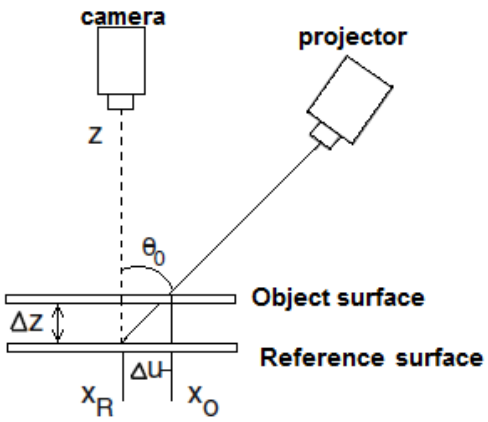

Figure 13- Moiré Fringe experience used in this study

Typical images obtained by this method can be seen in Figure 14. Comparing a surface before and after being tested, easily the deformation can be detected.

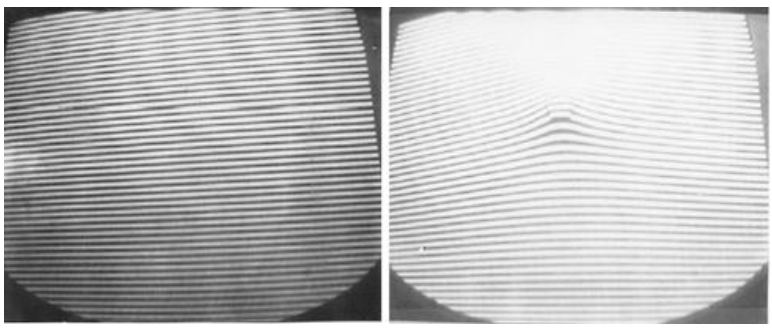

Figure 14-Comparison between reference surface (left) deformed surface (right), obtained by Moiré Fringes measuring technique.

The experimental setup of the Moiré Fringe method for ballistic impact on ceramic tiles is represented in Figure 15. The use of mirrors it for the protection of the flash tube so that it will not be damaged by debris caused by the impact.

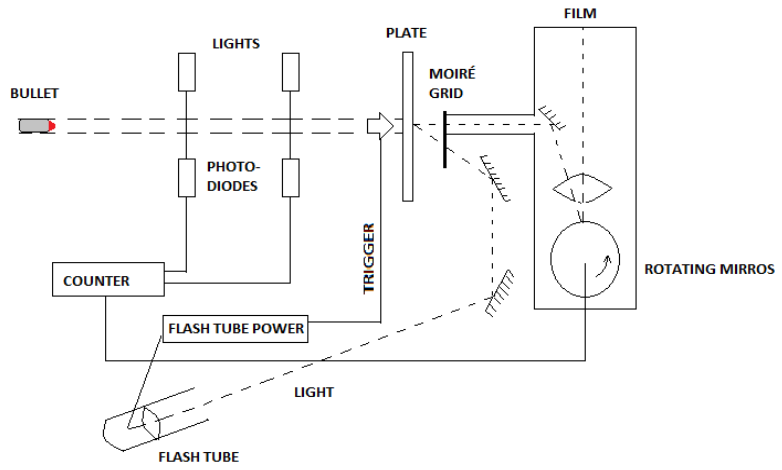

Figure 15- Experimental setup of Moiré Fringe employed in this study

In order to obtain correct and viable results, it is fundamental to assess the following parameters from (Beynet P. and Plunkett R., 1971):

a) Transverse dynamic equation

$$\frac{1}{r} = \frac{\partial}{\partial r}\left[r\,\frac{\partial Mr}{\partial r} + M_r - M_\theta + nN_r\,\frac{\partial w}{\partial r}\right] = 2b\rho\,\frac{\partial^2 w}{\partial t^2} \tag{3.11}$$

Where:

M_θ - Bending moment on circumferential surface

M_r - Bending moment on radial plane → máx= Yb^2

N_r - In-plane radial force intensity → máx Nr= 2Yb

Y - Yield stress

w - Transverse displacement

2b - Thickness of plate

ρ - Density

t - Time

r - Radius of the plane section

b) Force acting on the plate

$$2\pi r M_2 Y 2b\,\frac{\partial w}{\partial r} = (M_2 + \Delta M_2)\,\frac{\partial^2 w}{\partial t^2}\,atr \tag{3.12}$$

Where:

r_m - Radius of projectile

M_2 - Mass of projectile

ΔM - $\pi r^2 2b\rho$

c) Difference of the elevation between fringes

$$h = \frac{p}{tan\theta_1 + tan\theta_2} \tag{3.13}$$

Where:

p - Pitch of the moiré grid

θ_1 - Angle of incidence of the light

θ_2 - Viewing angle

d) Linear displacement, W, along the normal direction (Shepherd R. and Wenskley L. M., 1965) :

$$W = \frac{N \times p}{\tan\theta_1 \times tan\theta_2} \tag{3.14}$$

Where:

N - Fringe order

3.1.5. Shadowmetry

The amplification of an image is a hard technique when trying to avoid large expenses. Therefore, a simple game of shadows can be a possibility to have in mind. A shadow is basically an obstruction to a light beam produced by an object in its path.

Being the distance of the object to the screen, a, distance from the screen to the light source, d_1, the length of the light source, b, and dimension of the object in study, O, are the main influencers of the size of the shadow, S,. The equation that generates such parameter, S, is presented by Ditzhuijzen C.S.E., (October 2013):

$$S = \frac{a \times O}{d_1 - a} \times b \tag{3.15}$$

The main idea to implement this technique was that it is most difficult to combine micro precision (µm) with micro time (µs). Amplification of the micro precision to mm would minimize one of those two matters. Time could be solved by a high speed

camera, but small dimensions remains to be a problem. Considering previous studies Ditzhuijzen C.S.E., (October 2013), it is of easy comprehension that the first cracks in an alumina tile occurred about 4 μs after impact. Therefore, knowing a priori the approximate time of measurement to be effectuated, the image can be project on a second surface, amplifying the image, increasing, S, by equation (3.15). The Shadowmetry setup used for the experiment of ceramic tile deflection measurements is presented in Figure 16.

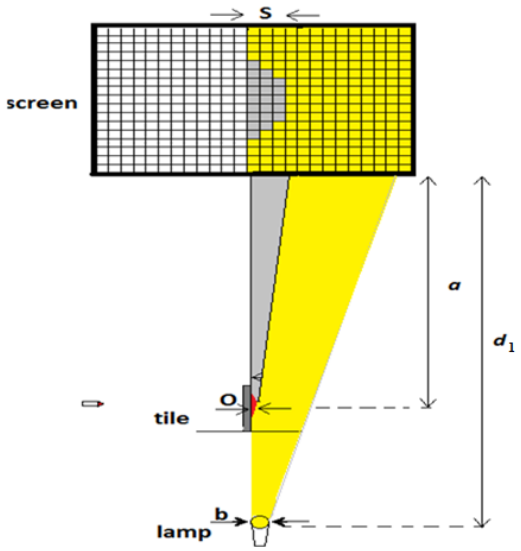

Figure 16- Shadowmetry technique setup scheme operated in this study

Using Figure 17, it is of easier comprehension to understand the behavior of shadows created by a light obstruction of a small object. The object size is considered to be infinitely small so that the light beam and the shadow provoked by the object have a triangular aspect.

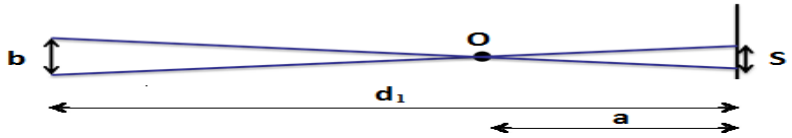

Figure 17- illustration model for calculations of the shadow size crated by an object obstruction

The size of the image can be calculated by the following equation:

$$\frac{b}{d_1-a} = \frac{s}{a} \leftrightarrow s = \frac{a}{d_1-a}\ b \tag{3.16}$$

The size of the object is enlarged with a factor:

$$\frac{s}{o} = \frac{d_1}{d_1 - a} \tag{3.17}$$

Calculating back to the real size of the object, the resolution of the image is given by:

$$\text{Resolution} = \frac{(3.16)}{(3.17)} \tag{3.18}$$

Therefore, in order to understand the above equations, an example was made by using the following parameters:

d_1=1.5m,
a=1.3m.
b=0.6mm

By using equation (3.16), the projected object size is:

$$s = \frac{1.3}{1.5-1.3} \times 0.6^{-3} = 0.0039 = 3.9mm$$

Concerning the size of the object enlargement (3.17), it will be enlarged with the factor:

$$\frac{d_1}{d_1 - a} = \frac{1.5}{0.2} = 7.5$$

Finally, the resolution of the image (3.18) is:

$$\frac{0.0039}{7.5} = 0.000502m = 520\mu m = 0.5mm$$

Thus, one can conclude that images with a size lower than $0.5\,mm$ will not be detected by shadowmetry, because of the image blur.

3.2. Electrical methods

As referred previously, also electrical methods could be used for measurement of the deflection of ceramic tiles during ballistic impact.

Among the known methods, the most commonly used electrical/magnetic methods assessed on this work were:

- Capacitive displacement sensors;

- Eddy Current displacement sensors.

3.2.1. Capacitive displacement sensors

Capacitive displacement sensors are composed of three components, two electrons and a dielectric. A probe that uses changes of capacitance to sense changes of thickness of the material, driver electronics that convert capacitance to voltage and a device to record voltage changes during the proses, (Catalogue, Physik Instrumente, 2007). Capacitive displacement sensors are used in several applications such as assembly of precision equipment, machine tool metrology and precision thickness measurements. They are non-contact devices that give accurate values of position measurements of conductive materials. By assembling a capacitive sensor on both sides of a plate or on two plates, the capacitance (Website R1) can be measured and, therefore, obtain the thickness of a plate or distance between to surfaces (Catalogue, Physik Instrument, 2007).

To measure capacitance between a reference surface and one that has been displaced. Antonelli K., et al. (1999), proposed the use of the following equation:

$$C = \frac{\varepsilon_0 \times K \times A}{d_2} \tag{3.19}$$

Where;

C – Capacitance

ε_0 – Permittivity of free space constant

K – Dielectric constant of material between plates

A – Area of plates

d_2 – Distance between plates

Capacitor displacement sensors use flat plates. Therefore, the deflection of the ceramic tile surface during ballistic impact will provoke an error capable of ruining our precise measurements. Both sides of the plate should also be parallel to maximize accuracy. In flat parallel plates, the precision of this method can go up to 0,01mm (Website R2).

This method uses only conductive materials and ceramics do not have electrical conductivity. To avoid this obstacle, a metallic layer could be attached to the ceramic tile to give the electrical conductive properties required.

Capacitive displacement sensors require a clean environment so that the dielectric constant of material between plates is constant (Catalogue, Physik Instrument, 2007). With the projection of ballistic fragments, this value can be influenced during the analyses. Humidity of the air should also be controlled as it increases the dielectric constant of the material to be analyzed.

If the target surface is irregular / not smooth, capacitor sensors average over the area to be analyzed. In situations of large irregularities on the surface, an error estimate should be taken in counter during all calculations (Catalogue, Physik Instrument, 2007).

Figure 18 shows the probe approach to the target to be analyzed and a graphic of the evolution of the capacitance in order of the displacement.

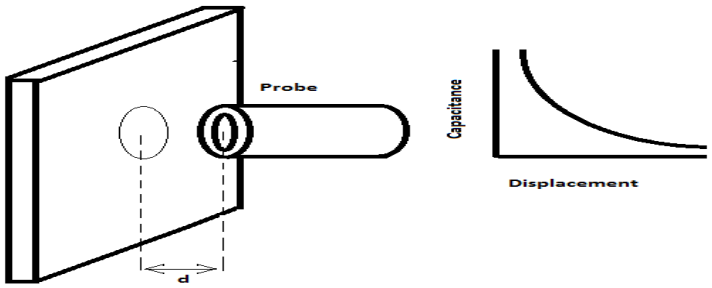

Figure 18- Capacitor displacement sensor

3.2.2. Eddy current displacement sensors

Eddy current displacement sensors are non-contact sensors that use magnetic fields to measure thicknesses, distances between objects and deformations (Lai Y., 2005). It is composed of a probe that produces a magnetic field that, when near a conductive material, creates electrical eddy-currents in the material. The electrical current produces a magnetic field that is opposite to the field of the sensor. The interaction between magnetic fields is used to measure distances between the material and the probe, using the following equation (3.20) that is Faraday's law of electromagnetic induction (Website R3):

$$\varepsilon = -\frac{d\phi_B}{dt} \tag{3.20}$$

Where:

$\boldsymbol{\varepsilon}$– Is the induced electromotive force

$\frac{d\phi_B}{dt}$ – The rate of change of magnetic flux.

Figure 19 shows how the probe acts with the target tile. The probe is connected to a driver that gives the excitation voltage (AC), does the signal processing, calibration and sets the output voltage/data.

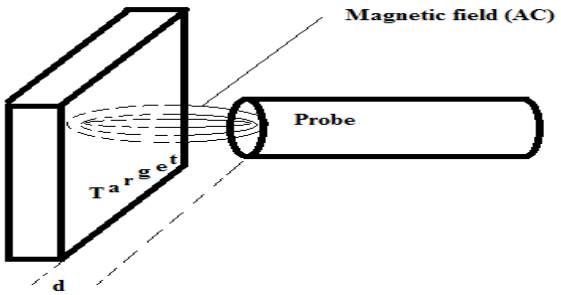

Figure 19- Eddy current Displacement sensor

The induced Eddy-current in the target material depends on the material properties such as, permeability and resistivity (Lion Precision, 2013). The depth of penetration of the magnetic field (Mook G., et al., 2006) is given by :

$$\delta = \frac{1}{\sqrt{f\mu\sigma}} \tag{3.21}$$

Where:

- δ– Penetration depth;
- **f**– Frequency;
- μ– Magnetic permeability of the material;
- σ– Electric conductivity of the material.

The magnetic field created by the probe, must penetrate the surface of the target in order to induce eddy currents in the material. The thicker the target is, the weaker will be the magnetic fields (Antonelli K., et al., 1999).

The strength of the eddy current and the resulting magnetic field depend on the permeability and resistivity of the material. Eddy-current sensors calibrated for nonmagnetic materials, ceramic tiles on our case, are not likely to function at all when used with magnetic materials. Eddy-current sensors should be calibrated to the same material as the target in the application and should not be used with rotating magnetic material targets unless the electrical errors are acceptable in the application (Antonelli K., et al., 1999).

Eddy-current sensors tolerate dirty environments, are relatively cheap in comparison with capacitor displacement sensors and have accuracy up to 0,05mm and the analog output time is 15μs (Lion Precision, 2013).

In this work, this wouldn't be a good option given the maximum of 0,05 mm of precision, the analog output time of 15μs when we need under 10μs, and for the fact that the probe needs to be close to the tile during ballistic impact, leading to damage and high replacement costs.

In conclusion, the main advantages and disadvantages of each measuring technique to obtain the deflection of a ceramic tile during ballistic impact are summarized in Table 2. The deflectometry method is simple, yet effective and accurate for optical measurements of a dent on a plate.

Table 2- Pros and cons of each technique

Technique	Pros	Cons
DIC and High speed camera	✓ Accuracy up to 0,01 mm.	× Spickles are required. × Expensive accurate scan machine required. × Definition of all parameters accurately .
Deflectometry	✓ Accuracy up to 0,010 mm. ✓ Simple and low cost equipment. ✓ No new equipment required. ✓ Simple calculations .	× Precision of the experiment settings. × Assumption of the shape of the dent to be spherical.
Newton rings	✓ Low cost equipment. ✓ Precision up to 0,015 mm.	× Never tested in Ballistic environment. × Static tests not conclusive. × Difficulty of measuring the rings captured by a high speed camera.
Moiré Fringes	✓ Precision up to 0,01 mm. ✓ Low cost equipment. ✓ All calculations explained in detail.	× Complex experiment setup. × Little background information about passed experiments.
Shadowmetry	✓ Low cost experiment. ✓ Easy Calculations. ✓ Simple output data.	× Blurriness of the image. × Low precision. × Selection of correct beam of light/laser.
Capacitive sensors	✓ Accuracy up to 0,01 mm. ✓ Non-contact device.	× Requires electrical conductive material.. × Requires clean environment. × Not functional in ballistic conditions. × Expensive equipment.
Eddy-Current sensors	✓ Functional in dirty environments. ✓ Not influenced by impact wave.	× Analog output time of 15µs is under wanted. × Accuracy of 0,05mm. × Approximation between probe and tile.

4. RESULTS AND DISCUSSIONS

After analyzing all options of measuring techniques to obtain the values of deflection of a ceramic tile during ballistic impact, a series of static experiments were performed. The objective of these experiments was to prepare a future dynamic situation experiment. Due to the costs of the assessment of a dynamic experiment, it is important that all possible situations are analyzed to avoid surprises that cost time and money.

4.1. Static Deflectometry experiments

Before beginning static experiments of ceramic materials, a metallic material was used due to its reflective properties. Two dents were made on two brass plates with 100×100mm dimensions and 3mm thickness. The choice for a brass plate was due to the reflective properties when polished, acting as a perfect mirror. The plates were dented using a 25mm Ø steel sphere and a press. The heights of the dents were measured with a precision dial gauge (Figure 20).

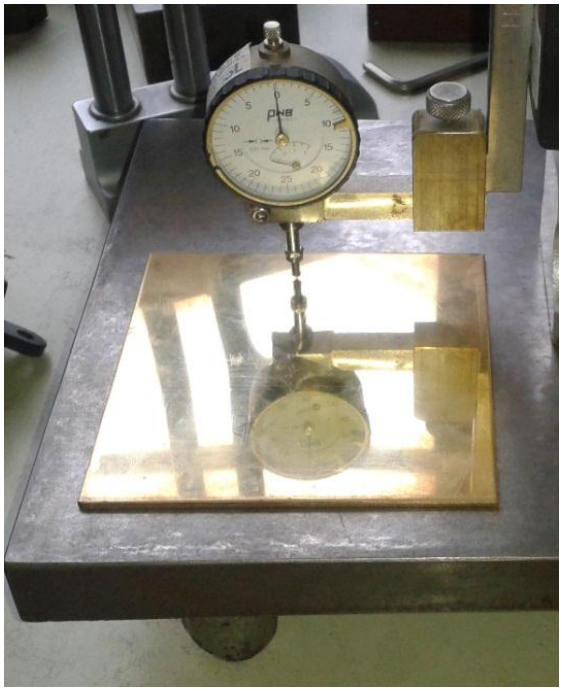

Figure 20- Precision Dial Gauge applied to a brass plate

An experimental setup as shown in Figure 21 was used to measure the height of the dents using deflectometry. This set up was assembled at a workshop at the TNO facilities where all necessary material was provided. The grid was obtained by a polycarbonate plate, where straight common thick lines distanced by 10 mm to be reflected on the brass plate were designed.

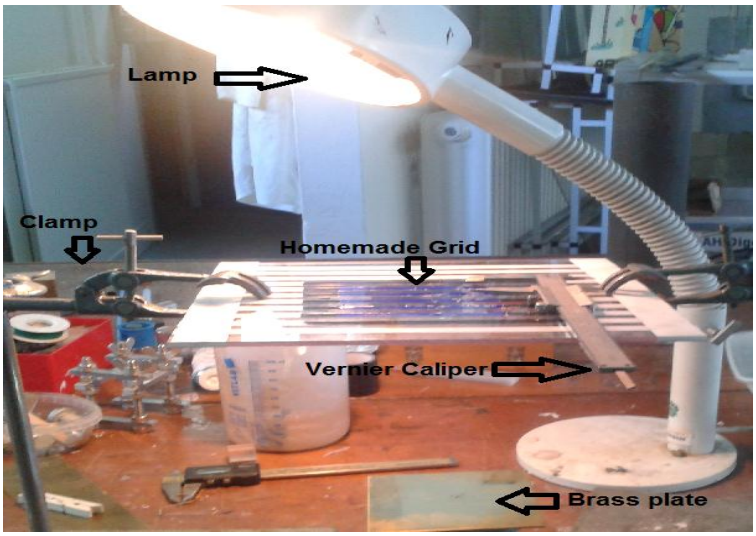

Figure 21- Optical experiment for deflectometry

Two dents were made using the press machine. One with a dent width, Ø = 27mm and another with Ø = 42mm. The dent height, x, were of 0.12 and 0.42mm respectively. The mechanical measurements, using the measuring gauge, are provided in Table 3.

Table 3- Dial Gauge measurement of maximal height of dents in brass plates

	Ø=27mm dent	Ø=42mm dent
Precision Dial Gauge measurement ,x, (mm)	0.12	0.42

The image reflected on the brass plate surface can be seen and measured without using any amplification device. Figure 22 shows the distortion of the grid lines, observed on the brass plate reflective surface, caused by the dent on the plate. In order to obtain the dent size, x, using the deflectometry method, it is necessary to measure the additional parameters such as, distance between the grid and the brass plate, d_0, the object size, o, that corresponds to the number of lines deformed multiplied by the distance

between the lines on the grid (10mm), and also the size of the image deformed, I, on the brass plate. In this work we chose to vary the distance, d_0, keeping the other parameters, o, and, I, constant.

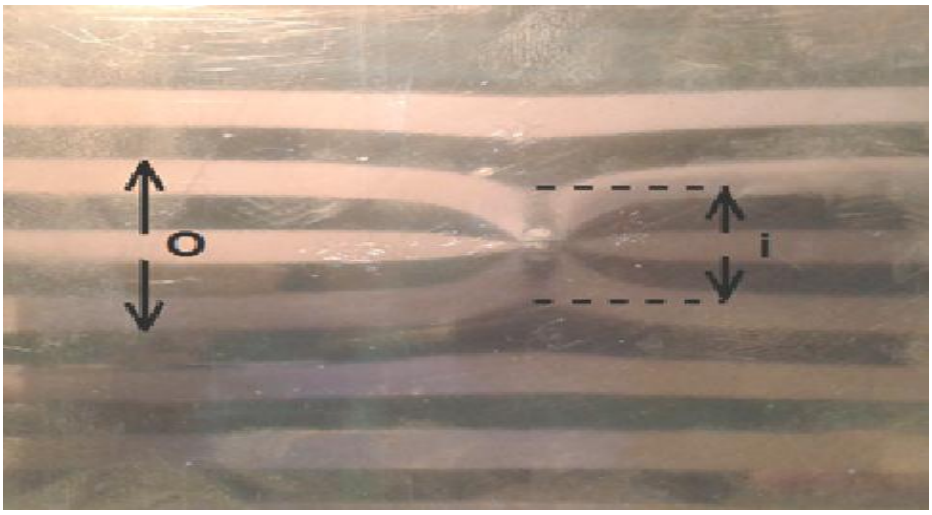

Figure 22-Example of a reflected image deformation of the brass plate

This procedure was used with a metallic brass plate, as well as two different ceramic materials, Al_2O_3 and SiC. The results are grouped during the next subsections for each material.

4.1.1. Brass material results

Using equation presented in the previous chapter, (3.1) to (3.4), we can calculate the height of the dent, x, using an Excel sheet. The results obtained for Ø=12 and Ø=14mm are tabulated in Table 4 and 5 respectively. Analysing both tables, it is possible to conclude that the error increases with the distance, d_0, between the grid and the brass plate. The reflection becomes more blurry and irregular. This characteristic influences the accuracy of the results to be analysed. It is imperative to have clear images due to the reflective surface. If this characteristic is not perceptible, the use of deflectometry in order to study spherical deflections is impossible.

Table 4- Optical measurements using deflectometry method of a mechanically measured 0.12 mm dent size on a brass plate

Distance d_0(m)	Dent size x(mm)	Dial Gauge measured (mm)	Deviation (mm)	Error %
0.28	0.06	0.12	-0.06	-49
0.27	0.06		-0.06	-48
0.24	0.07		-0.05	-42
0.20	0.08		-0.04	-35
0.19	0.10		-0.02	-15
0.17	0.09		-0.03	-26
0.16	0.10		-0.02	-15

Table 5- Optical measurements using deflectometry method of a mechanically measured 0,42 mm dent size on a brass plate

Distance d_0 (m)	Dent size x (mm)	Dial Gauge measured (mm)	Deviation (mm)	Error %
0.28	0.12	0.42	-0.30	-71
0.27	0.12		-0.30	-70
0.24	0.15		-0.27	-65
0.20	0.15		-0.27	-64
0.19	0.15		-0.27	-64
0.17	0.16		-0.26	-62

The evolutions obtained for both case studies are presented in Figures 23 and 24. The results show a large error % that can be justified either by the irregularity of the dent shape or by the deformed grid lines.

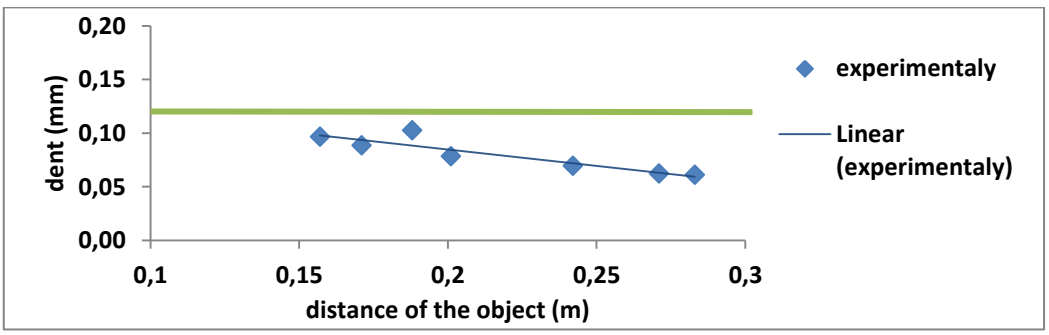

Figure 23-Graphic result analyses of deflectometry on a mechanically measured 0.12mm dent size on a brass plate

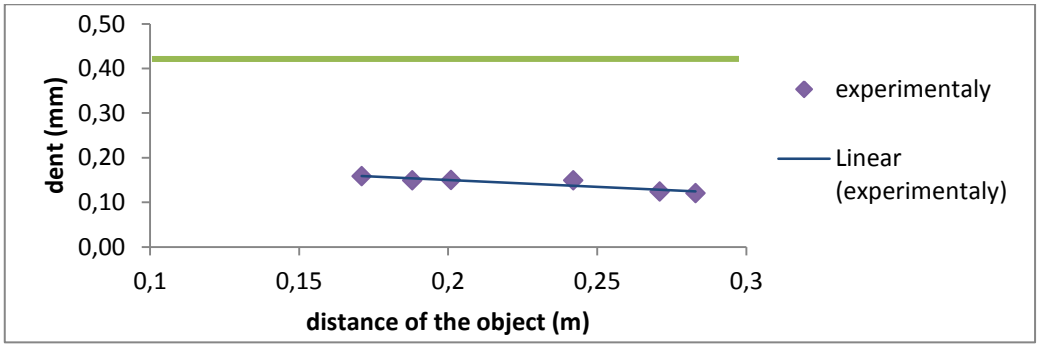

Figure 24-Graphic result analyses of deflectometry on a mechanically measured 0.42mm dent size on a brass plate

The values obtained with the 0.12mm dent height are more accurate than those for dent height of 0.42mm. This is probably due to the imperfection of the spherical shape with increasing dent size. We can analyse this experiment assuming the properties of a convex mirror, once a perfectly spherical dent is assumed.

Next, a plastic grid was made in Excel and printed on a transparent sheet and subsequently glued on a transparent plastic plate, with all lines 4mm thick and 4mm apart. Using this new grid with smaller lines, the accuracy of measurements increases.

In order to evaluate the results during ballistic impact, where only images of a ceramic tile during impact can be obtained. A picture of the brass plate was taken to get all data needed and that are perceptible optically without using any device as shown in Figure 25.

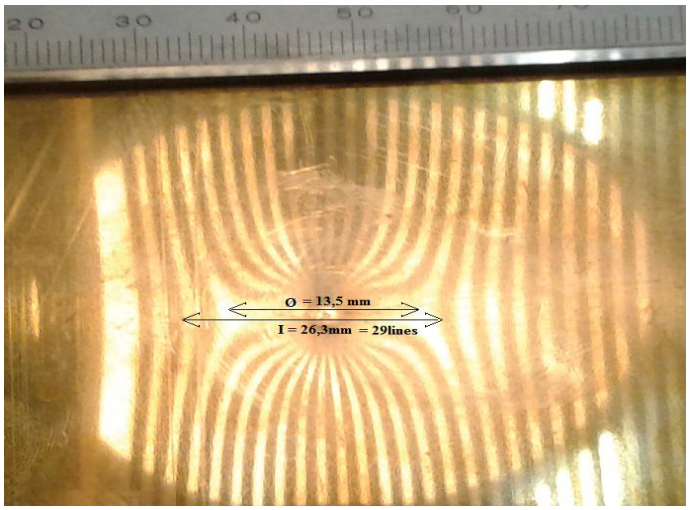

Figure 25-Experimental Deflection measurement on a brass plate

The Virtual image size, I, is the distance between several deformed lines from the grid reflection on the reflective surface. The number of lines to consider is irrelevant once that the objective is to compare a distorted and undistorted image. It is measured on the tile image with the help of a scale that must be on the tile. The object size, o, is obtained by multiplying the number of lines measured in, I, by the thickness of the lines on the grid. It is important to understand that the virtual image I must be measured using the reflected image on the tile surface and the object size o is measured on the grid. At this moment, the dent diameter, Ø, is not perfectly clear. Therefore, it was measured mechanically to better understand the image behaviour and by analysing Figure 25, it is perceptible that the dent diameter can be measured by half the distance between the last continuous line and the first discontinuous one (Ø= 13.5mm).

The image in Figure 25 is from a brass plate, 3mm thick, distanced 322 mm from the reflected image, do, the Virtual image size, I, is 26.2mm, the Object size, o, is 29 lines × 4mm =116 mm and the dent diameter, Ø, has the value of 13.5mm.

Using previous equations (3.1) to, (3.4), of chapter 3.1.2. we obtained the results presented in Table 6.

Table 6- Mechanical and Optical Measurement of a brass plate

Mechanically measured 0,12mm dent					
Image	I	2.62E-02	m	Output	
Object	o	1.16E-01	m	Input	
Number of lines of the virtual image	n	29			
Distance between lines on grid	g	4.00E-03	m		
Distance of the object	d_0	3.22E-01	m		
Virtual distance	d_I	7.27E-02	m		
Focal point	f	5.93E-02	m		
Radius	R	1.19E-01	m		
Dent diameter	Ø	1.35E-02	m		
Dent radius	Ø/2	6.75E-03	m		
Dent size (optical)	x	1.92E-04	m	0.19	x(mm)
Measured mechanically	x	1.20E-04	m	0.12	x(mm)
Error %				**60**	**%**

As to be concluding, the optical dent size, x, is of 0.19 mm. This result is higher than the mechanically measured 0.12 mm ± 0.010mm. It is important to have in

mind that this technique will only be accurate in a perfectly spherical dent (Feyman R., 1963), which was not the case.

4.1.2. SiC material results

In order to validate the results, the experiment was repeated using the same setup and dimensions but with a ceramic SiC 100 × 100 mm and 5mm thick tile. The objective was to simulate the real dynamic deflection by using a drop of epoxy glue, resembling a dent with mechanically measured, Ø, value of about 20mm.

A problem with SiC tiles, is the absence of reflective properties. To solve this disadvantage, two solutions could be adopted. Either the SiC surface could be polished influencing the material properties, or a coating could be created for the ceramic surface. Therefore, and so that the mechanical properties of the SiC tiles were not influenced, a coating was made using a transparent polymer *Splitterschutz foil 115µm height* giving the non-reflective surface of the ceramic tile reflective to light.

This way, it was possible to study the reaction of the coating on the measuring technique in a very similar situation as to be observed during ballistic impact. Figure 26 shows a picture of the dented reflection on the surface of the ceramic tile with (left) and without (right) the coating.

It is visible that with the coating it is possible to visualise the grid lines being reflected on the coating attached to the ceramic tile. On the other hand, without coating, this technique would be impossible on ceramic tiles. This was a major step for the success of this technique applied to the study of ceramic tile deflection during ballistic impact.

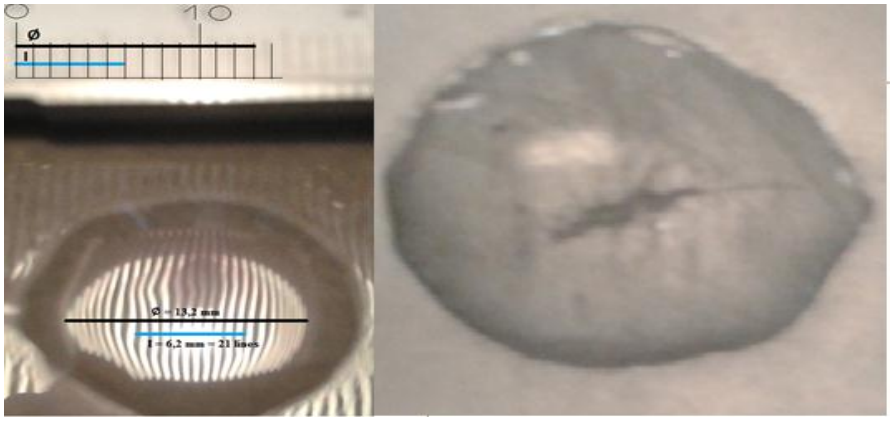

Figure 26-SiC reflective surface with (left) and without (right) polymer coating

Using equations (3.1) to (3.4) from chapter 3.1.2 coupled to the data showed on Figure 26, the resulting is compiled in Table 7.

The error is of 20% less than the 60% on the brass plate (Table 6). This is based on the fact that the dent diameter is visible and the dent is more spherical.

Table 7- Mechanical and Optical Measurement of a dent on a ceramic SiC tile

Mechanically measured 0,41mm dent					
Image	I	6.20E-03	m	Output	
Object	o	8.40E-02	m	Input	
Number of lines of the virtual image	n	2.10E+01			
Distance between lines on grid	g	4.00E-03	m		
Distance of the object	d_0	3.22E-01	m		
Virtual distance	d_I	2.38E-02	m		
Focal point	f	2.21E-02	m		
Radius	R	4.43E-02	m		
Dent diameter	Ø	1.32E-02	m		
Dent radius	Ø/2	6.60E-03	m		
Dent size (optical)	x	4.95E-04	m	0.50	x(mm)
Measured mechanically	x	4.10E-04	m	0.41	x(mm)
Error %				**20**	**%**

It was also decided to make a new static experiment involved a Nikon D300 digital camera. By this way, it was possible to make the focus manually. Using the SiC ceramic tile, a single picture for all data collection. The setup used in this experiment is schematically presented in Figure 27. With G being the grid, T the tile and C the Camera, this was the most similar setup as possible to the ballistic experiment.

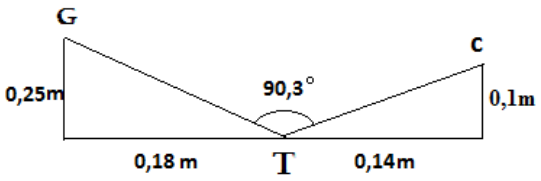

Where:
G- Grid
T- Ceramic tile
C- Camera

Figure 27-Experimental setup of the position of the components necessary for the Deflectometry experiment

It is important to notice, that this experimental designs are most similar to the ballistic tests, which were made at the ballistic offices of TNO.

Figure 28 shows the picture of the ceramic tile to be analysed. The blurriness of the image is due to the distance between the camera and the ceramic tile, as well as the distance between the grid and the tile. The dent diameter, Ø, is the most difficult to measure. The brightness of the image, can make measurements easier, therefore it is important to analyse the source of light influence on the pictured tile.

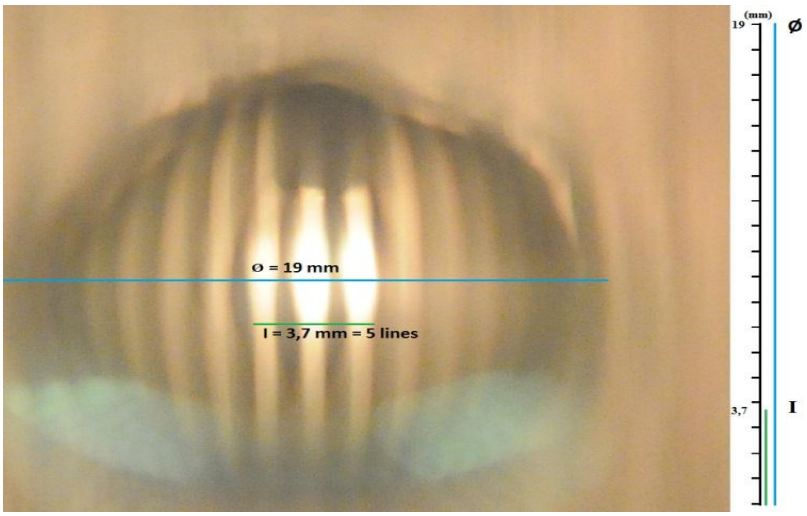

Figure 28-Deflection measurement on the SiC ceramic tile

The Excel sheet results are given in Table 8 and show that although the accuracy is not yet as expected, the method could be used and applied in any situation, due to its simplicity.

Table 8- Mechanical and Optical Measurement of a dent on a ceramic SiC tile

Mechanically measured 0,41mm dent					
Image	I	3.70E-03	m	Output	
Object	o	1.60E-02	m	Input	
Number of lines of the virtual image	n	4.00E+00			
Distance between lines on grid	g	4.00E-03	m		
Distance of the object	d_0	2.00E-01	m		
Virtual distance	d_I	4.63E-02	m		
Focal point	f	3.76E-02	m		
Radius	R	7.51E-02	m		
Dent diameter	Ø	1.90E-02	m		
Dent radius	Ø/2	9.50E-03	m		
Dent size (optical)	x	6.03E-04	m	0.60	x(mm)
Measured mechanically	x	4.10E-04	m	0.41	x(mm)
Error %				**47**	**%**

The dent diameter can be seen and measured using Figure 28. It couldn't be seen on the brass plate but is perceptible on the epoxide glued dent on the SiC tile.

In order to study the influence of each optical parameter, the image size, I, the object size, o, and the dent diameter, Ø, were changed 1mm and 90% of their value, using Table 9 as reference. Furthermore, Table 10 was compiled using the data obtained by those changes.

Table 9- Mechanical and Optical Measurement of a dent on a ceramic tile using a Grid with 8mm lines

Mechanically measured 0,56mm dent					
Image	I	4.50E-03	m	Output	
Object	o	7.20E-02	m	Input	
Number of lines of the virtual image	n	9			
Distance between lines on grid	g	8.00E-03	m		
Distance of the object	d_0	2.30E-01	m		
Virtual distance	d_I	1.44E-02	m		
Focal point	f	1.35E-02	m		
Radius	R	2.71E-02	m		
Dent diameter	Ø	1.10E-02	m		
Dent radius	Ø/2	5.50E-03	m		
Dent size (optical)	x	5.65E-04	m	0.57	x(mm)
Measured mechanically	x	5.60E-04	m	0.56	x(mm)
Error %				**1**	**%**

Table 10 shows that the virtual image, I, and the dent diameter, Ø, are the parameters of larger influence in the results. Therefore, it is important to be as cautious as possible when registering these values. The object size, o, is not as influencing as the virtual image and the dent diameter, but also easier to measure once that it represents the number of lines deformed multiplied by their thickness on the grid.

Table 10- Image ,I, Object ,o, and dent width , Ø, influence on Deflectometry measuring technique

	Reference (mm)	**Influence value (mm)**	**Influence percentage (%)**
I + 1mm	0.57	0.47	17
o + 1mm	0.57	0.57	2
Ø + 1mm	0.57	0.67	20
90% I	0.57	0.63	12
90% o	0.57	0.51	9
90% Ø	0.57	0.46	18

Next, 3 setups were analysed (Figure 29) with various angles between the camera and the ceramic tile **α,** between the grid and the ceramic tile **β** and also the angle between the grid projection and the camera focus on the tile **γ.** Three different angles of **γ** were selected using values from 80-110º and the results are compiled in Table 11. It is also important to understand that each angle of γ, refers to a colour named by A, B and C on table 11.

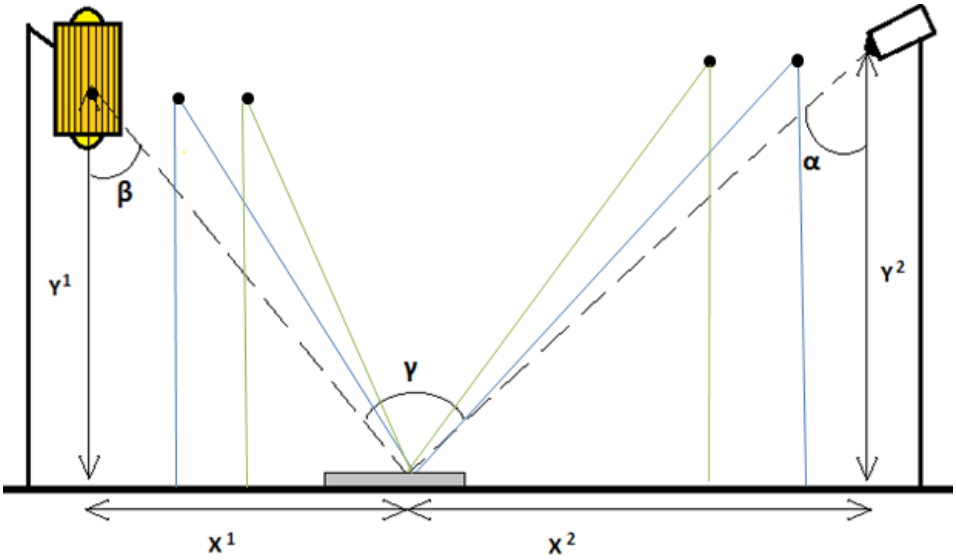

Figure 29- Analyses of the influence of the position of the grid and camera on the measurement results

Table 11 was elaborated to understand the influence of the angle of each component (camera and grid), in the results of this measuring technique. An important conclusion can be obtained, that is, the larger **γ** is, the larger will be the error.

Table 11- Results of the influence of the position of the camera and grid during measurements

	ϒ (°)	**error %**
A	101	20
B	96.3	19
C	89	15

4.1.3. Al_2O_3 material results

In addition to SiC tiles, also other ceramic was used, the Al_2O_3. This is due to the fact that alumina tiles are frequently used as a frequent material in ballistic impact

studies. An alumina (Al_2O_3) tile with white colour was used to analyse the reflection properties. The result is Figure 30 where we can see an image of the Al_2O_3 tile (left) and the SiC tile (right) showing that the Al_2O_3 surface is also reflective when in use of the coating. The customized coating, a self-adhesive polymer foil served its purpose well on the dark surface of the SiC tile but also on the white Al_2O_3 surface. To improve the adhesive properties, a thin film of water covered the surface of the ceramic tiles between the ceramic surface and the polymer. Using a oven to dry the water, the polymer adapted perfectly to the ceramic tile.

Both Al_2O_3 and SiC are relevant armor ceramic types, hence they both need to be analysed. The idea was to compare the reflective properties in ceramics with different surface colours. The SiC in black and the Al_2O_3 is white.

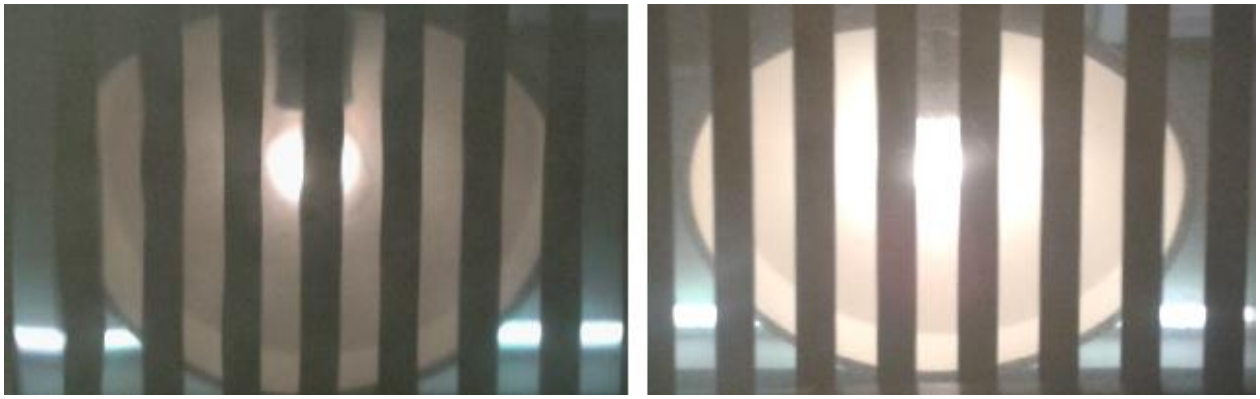

Figure 30- Reflective properties of the coating on Al_2O_3 (right) and SiC (left) tiles

Next, static measurement tests were performed using images obtained by a Shimadzu high speed camera which has a rather low pixel resolution 312×260 pixels. The objective was to confirm that the high speed imaging was accurate enough for this measuring technique. Figure 31 shows the setup of the static experiment using deflectometry method.

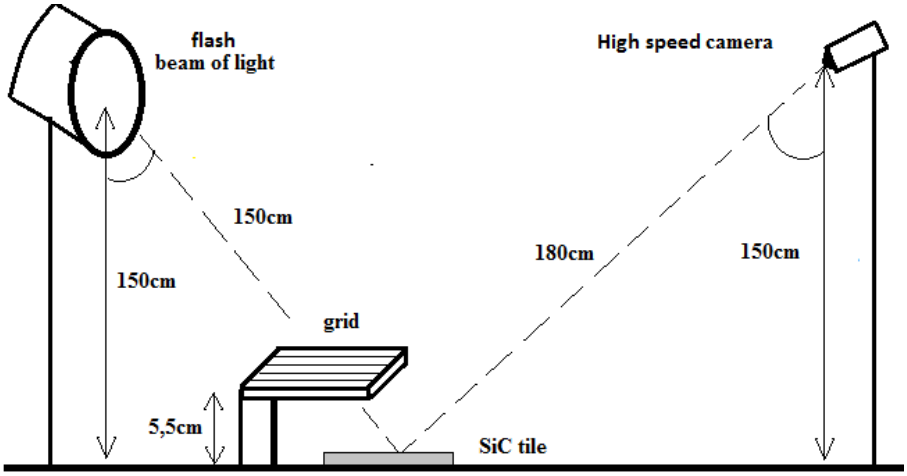

Figure 31- Experimental setup using high speed video

We used a Shimadzu high speed camera with the diaphragm maximally opened and an inter-frame time of 1 µs (a frame rate of 1 MHz) with 300mm zoom, one flash 500 Joule pulse in about 1 ms with a diffusor sheet light and a grid with all lines separated 4mm from each other. The first point to be analysed was the perception of the grid reflection on both the Al_2O_3 and SiC tiles represented in Figure 32. The reflection was perceptible and clear on both tiles.

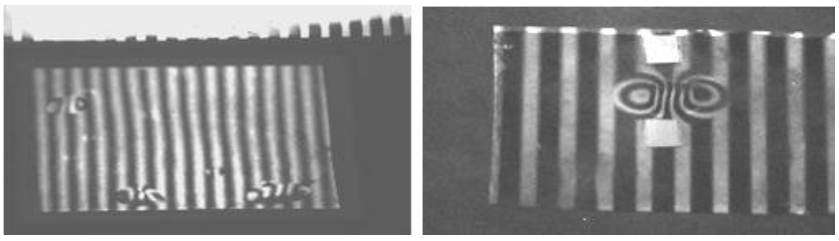

Figure 32- Al_2O_3 and SiC reflective surface obtained with Shimadzu high speed camera and 300mm lens

Next, using the dent with a 1,1cm diameter indent and mechanically measured indent height of 560µm on the SiC tile, it was necessary to increase the camera zoom to 600mm using a 2 times converter in order to analyse the reflected lines on the dent. The image obtained was Figure 33 that shows the projected lines being deformed where the dent was made. The dent diameter, Ø, is considered to be the distance between the centre of both circles visible in Figure 33. A diffusive material was adapted to the grid in order to homogenise the light intensity.

All equipment to be used during ballistic tests was confirmed to be accurate providing positive results.

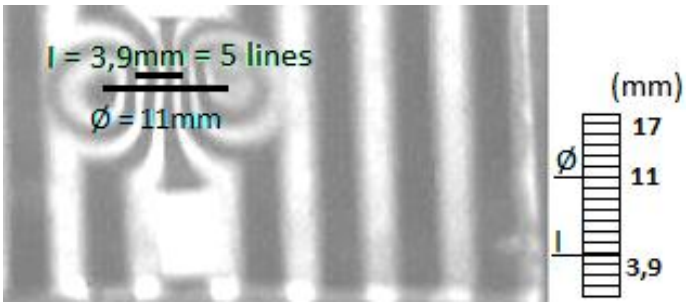

Figure 33- SiC tile Shimadzu image of a 0.56mm dent

Table 12 shows the results obtained from the analysis of Figure 33. The dent size, x, of the Al_2O_3 tile was obtained by deflectometry method.

Table 12- Mechanical and Optical Measurement of a 0.54mm dent on a SiC tile using a Shimadzu high speed camera and a Grid with 4mm lines

Mechanically measured 0,54mm dent					
Image	l	3.90E-03	m	Output	
Object	o	2.00E-02	m	Input	
Number of lines of the virtual image	n	5			
Distance between lines on grid	g	4.00E-03	m		
Distance of the object	d_0	6.00E-02	m		
Virtual distance	d_I	1.17E-02	m		
Focal point	f	9.79E-03	m		
Radius	R	1.96E-02	m		
Dent diameter	Ø	1.10E-02	m		
Dent radius	Ø/2	5.50E-03	m		
Dent size (optical)	x	7.88E-04	m	0.79	x(mm)
Measured mechanically	x	5.60E-04	m	0.54	x(mm)
Error %				**46**	**%**

All experiments done until this moment where using an epoxy glue drop as dent on a SiC tile and a pressed dent in a brass plate. Next, a new epoxy glue dent was made on an alumina (Al_2O_3) tile to study the response of this technique on this white surface ceramic material. The dent was measured mechanically with the precision dial gauge and had a height x of 0.28mm ± 0.01 mm. This epoxy glue dent was dried with the

tile upside down. The reason of this position was so that the excess glue would drop of the tile by gravity force during the dying process, and this way the drop would assemble to a spherical shape as necessary for deflectometry technique. The deflection measurement of the Al_2O_3 tile is showed in Figure 34. As can be seen, the Ø is about 2,2cm.

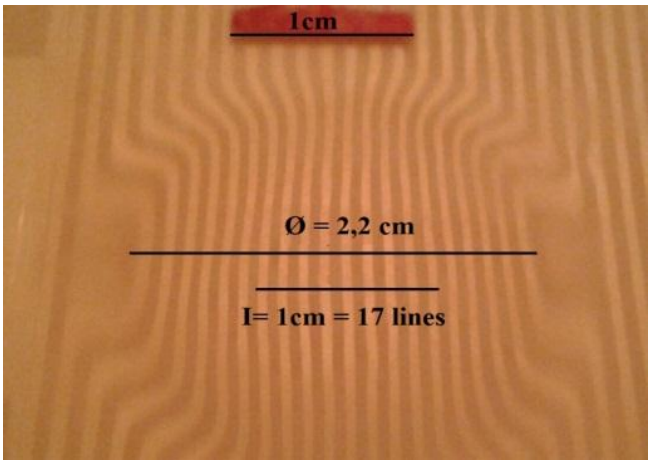

Figure 34- Deflection measurement on a ceramic tile Al_2O_3

Thus, all mechanically and optical data for this ceramic is listed in Table 13.

Table 13- Mechanical and Optical Measurement of a dent on a ceramic Al_2O_3 tile using a grid with 2mm width of grid lines

Mechanically measured 0,28mm dent					
Image	I	1.00E-02	m	Output	
Object	O	3.40E-02	m	Input	
Number of lines of the virtual image	N	17			
Distance between lines on grid	G	2.00E-03	m		
Distance of the object	d_0	9.80E-02	m		
Virtual distance	d_I	8.33E+02	m		
Focal point	f	9.80E-02	m		
Radius	R	1.96E-01	m		
Dent diameter	Ø	2.20E-02	m		
Dent radius	Ø/2	1.10E-02	m		
Dent size (optical)	x	3.09E-04	m	0.31	x(mm)
Measured mechanically	x	2.80E-04	m	0.28	x(mm)
Error %				**10**	**%**

The main conclusion to be drawn in that the error obtained is quite small, only 10%. In comparison with SiC and brass, this is an optimal result. A possibility to explain the difference between these results was studied in order to achieve a conclusion. The colour of the tile is irrelevant once that both are using the same reflective coating on the dent surface. The mechanical properties of the different materials do not influence the reflective property that is the only one that is relevant for all calculations. The dent dimensions of both tiles were different. The first thing to be noticed is the diameter of the dent of 1,1cm on the SiC tile and of 2,2cm on the Al_2O_3. This difference can also influence the shape of the dent which is a factor of large importance in the results as the shape of the dent is assumed to be spherical. It was necessary to know the shape of both dents in order to draw any conclusions. This was achieved using a precision measuring gauge that gave the different sizes during the diameter of each dent profile. Figure 35 shows the SiC real shape measured mechanically using the precision measuring gauge during the dent length, and the assumed by the deflectometry method. Analysing Figure 35, where the real shape and the assumed by the program are represented, it can be concluded that the dent on the SiC tile is not spherical but almost flat on its surface.

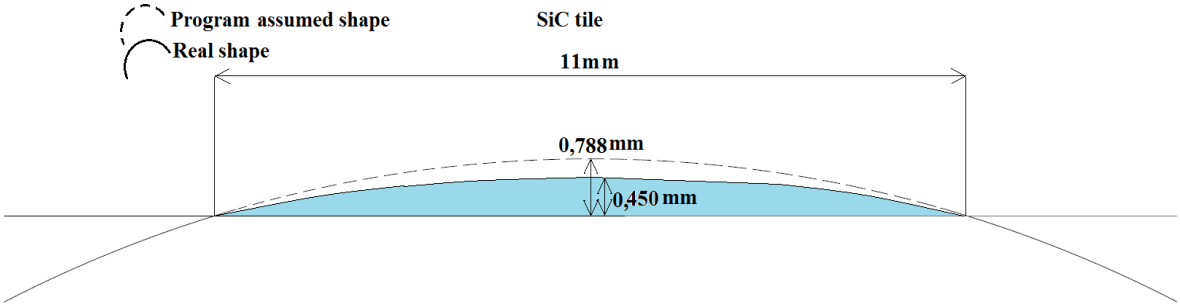

Figure 35- Real and program assumed SiC dent shape.

The irregular shape of the dent, influences the results giving a large error. This justifies the results of Table 13 once that the program analyses the diameter of the dent assuming a spherical surface what would lead to a larger dent size **x**. The shape of the dent on the Al_2O_3 is closer to the spherical shape explaining the more accurate results. The real shape and the shape assumed by the program are identical and more accurate results are obtained (error of 10%). This technique can only be able to generate the dent size **x** if the ballistic experiment approximates to a spherical dent.

4.2. Dynamic Deflectometry Experiments

To measure the tile deflection in dynamic experiments, an experiment series was performed by impacting ceramic tiles with projectiles. The experimental setup is presented in Figure 36 showing side and isometric views. Two ceramic materials were used in this experiment:

- 100×100 mm Al_2O_3 (7mm thick)
- 100×100 mm SiC (8mm thick)

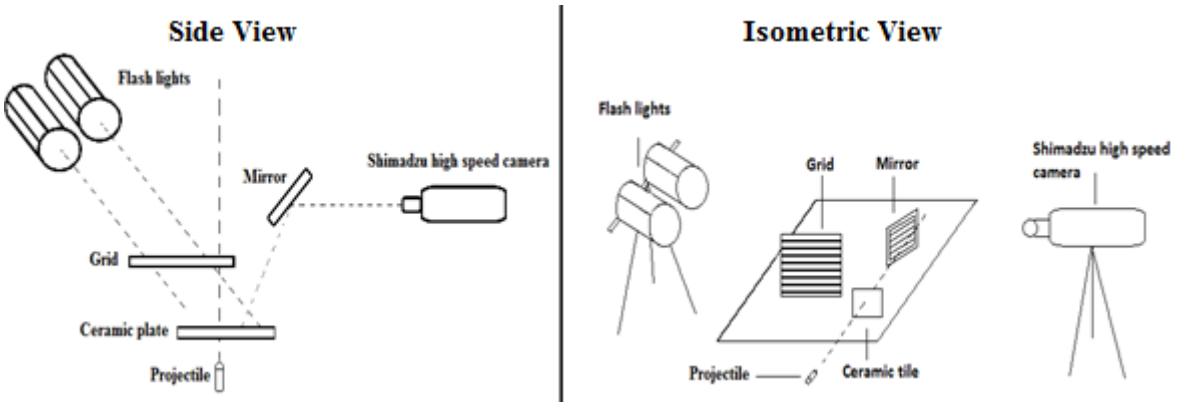

Figure 36-Side view (left) and Isometric view (right) of the experimental setup for the deflectometry experiment during ballistic impact

Both were submitted to ballistic tests using a bullet with the speed of 830 ±10 m/s. For this experiment series, a Shimadzu high speed camera was used with 300mm zoom and a 2 times converter giving the camera a zoom of 600mm. Two flash lights of 500Joule in about 1ms projected the grid lines on the tile. All lines on the grid were separated 2mm from each other and a diffuser was glued to the surface of the grid in order to diffuse the light provided by the flash lights. A series of twelve shots were performed. Six using Al_2O_3 and six with SiC tiles. For the tests on the Al_2O_3 tile, the gain of the camera was set at 15, lens diaphragm to 5.6 and time step to 1µs (1mfps). The camera settings for the tests performed on the SiC tiles were gain to 20, diaphragm to 5.6 and time step to 1µs. A mirror was used in order to decrease the distance between the high speed camera and the tile and that way get better resolution, decreasing the angle of camera view (Figure 29), blurriness of the projected lines from the grid on the ceramic tile without

having the high speed camera inside the shocking range. This will enable us to obtain clear images (shredding the mirror) without damaging the camera. A 10mm dot was applied on the rear in order to give us a scale on the tile. This will give us the possibility to measure the virtual image I that must be measured on the tile surface.

The objective of this setup was to obtain accurate data with low costs as the only things to be replaced between tests will be the polycarbonite grid, a mirror and a ceramic tile.

All data processing is using the same assumptions that the shape of the tile deflection is considered perfectly spherical. The frame analyses was treated as explained in section 4.1 with the only difference that we would measure the dent radius $\frac{Ø}{2}$ instead of the diameter Ø in order to decrease measurement errors.

In order to verify the assumption of a spherical dent during ballistic impact, Figure 37 shows the almost spherical dent shape with x=2.5mm. This information provides the confirmation that using deflectometry as a measuring technique for ballistic impacts on ceramic tiles is possible. Figure 37 also shows that the deflection provoked by a 7.62 APM2 bullet with a velocity of 830 ±10 m/s on a 100×100×7 mm Al_2O_3 tile is close to spherical. This optical measurement is only possible 14µs after impact because of the little image resolution for small dent sizes before this moment. This is in concordance to other previous results made in TNO and present on Figure 6, chapter 2.

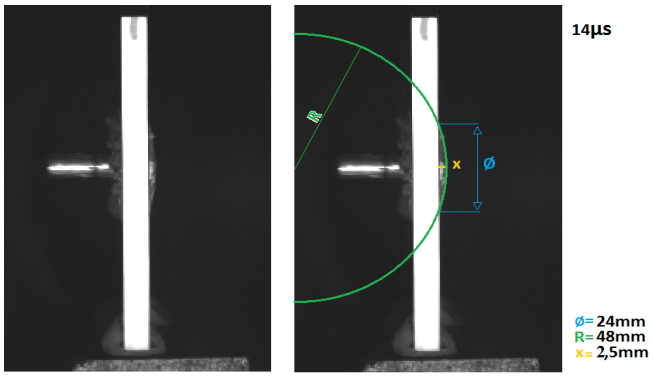

Figure 37- Side view of the deflection shape on a Al_2O_3 tile (7mm) during ballistic impact of a 7.62 APM2 bullet with a velocity of 830m/s at a time of 14µs after impact (Carton E.P. and Roibrocks R., 2012)

In order to use the deflectometry method to study the deflection on ceramic tiles, two different ceramics were subjected to the dynamic experiment; Al_2O_3 and SiC.

Both ceramics responses will be studied with a ballistic impact. All time references are considered to be from the moment the first deformations appear t_0 plus the time between frames until the moment to be analysed.

4.2.1. Al_2O_3 material results

As mentioned, the time step of the high speed Shimadzu camera was 1µs. In order to use this method, the reflective surface of the ceramic must be intact. Therefore, there will be a time when the damage on the reflective foil is such that the reflected lines from the grid are not clear anymore. Analysing Figure 38, it is possible to take some conclusions. From 1 to 5µs, the projected lines are deformed although it is difficult to observe. The deformation velocity is low. At 7µs, it is visible the formation of the first radial cracks. The reflected lines are deformed are perfectly perceptible. From 7 to 11 µs, the projected lines are easily distinguished between them. The moment of 13µs after impact, is the last moment when the deflectometry measuring technique is possible to be used, once that the lines projected are not distinguished one from the others. From this moment forward, the polymer coating is destroyed and this technique is not usable anymore.

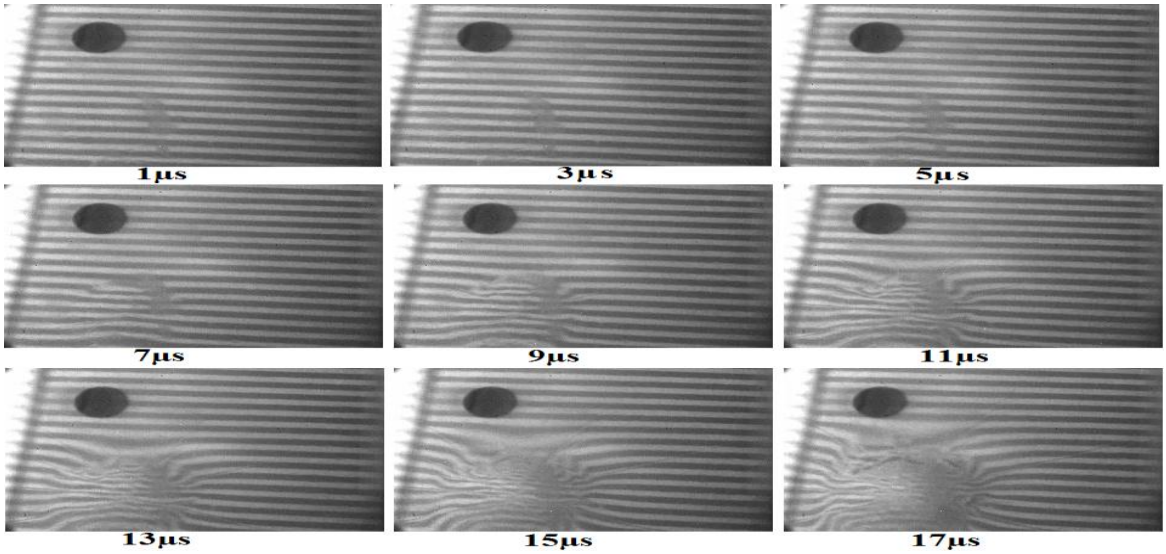

Figure 38- Different frames from projected lines on an Al_2O_3 tile during ballistic impact by a 7.62 APM2 bullet

In order to achieve deflectometry measurement results, each frame should be analyzed to obtain the value on the virtual image I by the distance between any number of

deformed lines, measured on the tile. The number of lines considered in I measurement, multiplied by the distance between the grid lines (2mm) provide the object size o. Finally, the radius of the dent $\frac{Ø}{2}$ is measured using the scale on the tile obtained by the 10mm circle. Figure 39 shows the 11µs frame with all values to be considered (I and $\frac{Ø}{2}$) in order to obtain the dent size x. The line distortion is perceptible on the rear of the impact surface. This figure is an example of how the data was treated for every 2µs in order to have conclusive results. Having in consideration that this technique has never been performed, there is no other work of comparison. All results must be then studied and analyzed so that this technique can be improved. The lines reflected on polymer coating of the ceramic tile are only perceptible to change/deform after 3µs. To improve this aspect, thinner lines could constitute the grid on a vertical direction. This way, the vertical thinner lines could be used under 5µs and horizontal thicker lines for further times.

.

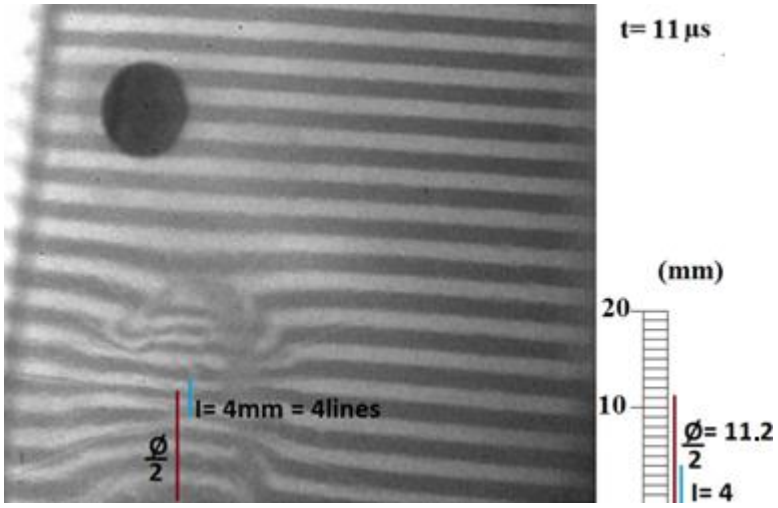

Figure 39- Image of a Al_2O_3 tile during ballistic impact by a 7.62 APM2 bullet using deflectometry method to measure the dent size x at 11µs

Table 14 shows the results obtained by the deflectometry Excel program at the 11µs moment in order to obtain the dent size x.

The dent radius, $\frac{Ø}{2}$, is given by the distance from the symmetry line in the axis of symmetry of the dent, to the last discontinuous line deformed.

Table 14- Dent calculation Excel sheet for a 7mm thick Al_2O_3 tile during ballistic impact by a 7.62 APM2 bullet using deflectometry method

15-06-54 experiment				**time**	**11µs**
Image	I	4.00E-03	m	Output	
Object	o	8.00E-03	m	Input	
I/o	M	5.00E-01			
Number of lines of the virtual image	n	4			
Distance between lines on grid	g	2.00E-03	m		
Distance of the object	d_0	8.30E-02	m		
Virtual distance	d_I	4.15E-02	m		
Focal point	f	2.77E-02	m		
Radius	R	5.53E-02	m		
Dent diameter	Ø	2.24E-02	m		
Dent radius	Ø/2	1.12E-02	m		
Dent size (optical)	x	1.15E-03	m	**1.15**	**x(mm)**

It is possible to see in Table 14 that the dent size x is of 1.15mm at a time of 11µs after the first deformation appears on the projected lines on the Al_2O_3 tile. Figure 40 shows the relation between the dent size and the time. It is perceptible that there is an almost constant dent increasing from 1 to 10µs. From this moment forward, the dent size increases with a different pattern. One justification for this behavior can be the fact of the smaller particles projected from the tile blast, are moving the polymer coating faster than the larger ones. To verify this assumption, Figure 41 was elaborated and relates the velocity of the deformation with the time. The velocity of deformation increases for the first 5µs, decreases between 5 and 9µs and there is a increment from 9 to 13µs. This variation of the velocity is possibly originated by a shock wave in the material, provoked by the ballistic impact. This is only an assumption, once that there isn't any work to compare results. These results complement the study elaborated by Carton E.P. and Roibrocks R., (2012) as they allow to measure deflections under 14µs. It is interesting to mention that using the same tile material and dimensions and same bullet velocity, the deflectometry method for 13µs gives a dent size x of 2.08mm and using the side-view method (Carton E.P. and Roibrocks R., 2012), for 14µs the dent size x is 2.5mm (see Figure 37). These results give credibility to both measuring techniques.

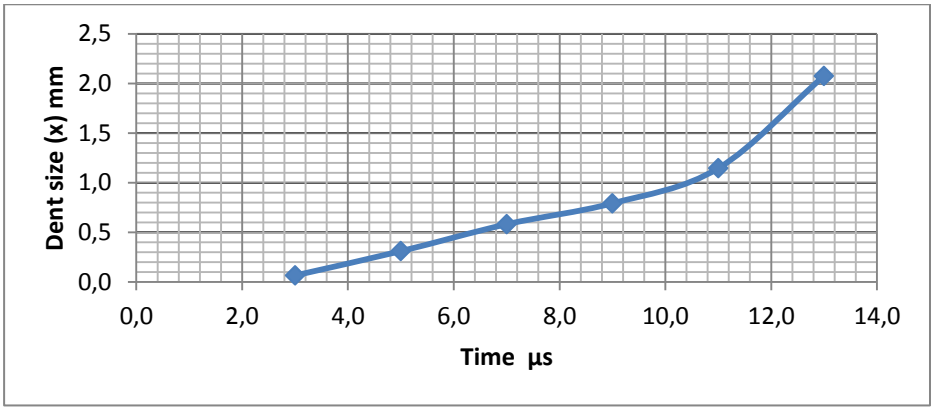

Figure 40- Relation between dent size (x) and time after impact of a 7mm Al_2O_3 tile during ballistic impact by a 7.62 APM2 bullet

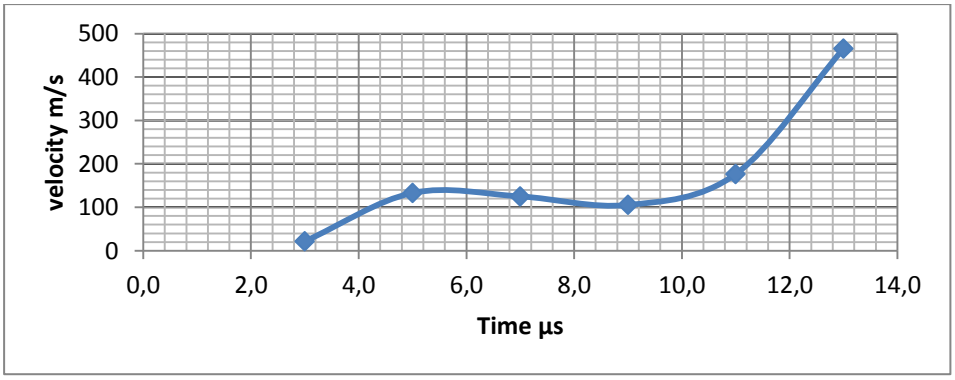

Figure 41- Relation between time after impact and deformation velocity of a 7mm Al_2O_3 tile during ballistic impact by a 7.62 APM2 bullet

Table 15 is a resume of the values from Figure 40 and 41. The objective of this table is to facilitate the analyses of data obtained by deflectometry measuring technique on Al_2O_3 tiles.

Table 15- Relation between dent size (x) and deformation velocity of a 7mm Al_2O_3 tile during ballistic impact by a 7.62 APM2 bullet

x(mm)	v(m/s)	time (µs)
0,07	22	3
0,31	133	5
0,58	125	7
0,79	105	9
1,15	177	11
2,08	465	13

4.2.2. SiC material results

The deflectometry measuring technique was repeated for SiC tiles with 100×100×8mm dimensions. Figure 42 shows the frame sequence from 3µs to 17µs with 2µs between frames. From 1 to 3µs the deformation is perceptible without any radial cracks visible. Analysing the 5µs frame, it is possible to see the first radial cracks (with the Al_2O_3 tile, this phenomenon occurred only at 7µs). The justification of the behaviour is related to the thickness of both tile materials (Al_2O_3 of 7mm and SiC of 8mm). The use of Deflectometry measuring technique is possible only until 13µs. After this moment, the polymer coating is destroyed and this technique is no longer possible. An equal behaviour was occurred with the Al_2O_3 tiles.

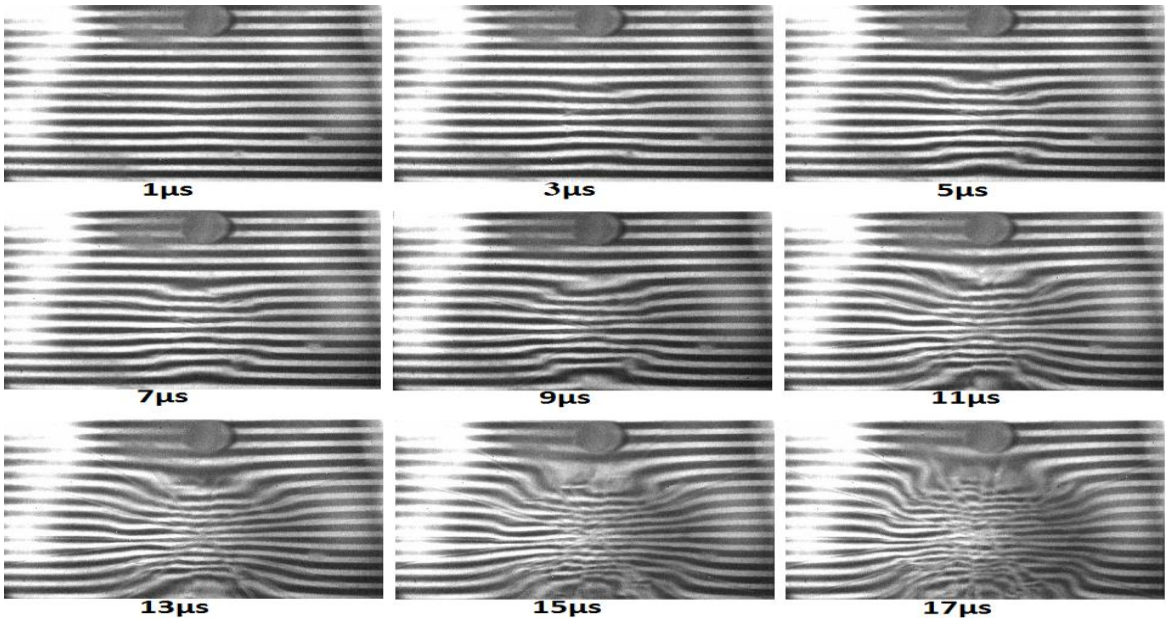

Figure 42- Different frames from projected lines on an SiC tile during ballistic impact by a 7.62 APM2 bullet

Figure 43 is a picture of the 11µs moment frame analysed to obtain the dent size, x, using deflectometry measuring technique. The radial cracks are present, as well as a projected line deformation used to measure the deflection using Deflectometry measuring technique.

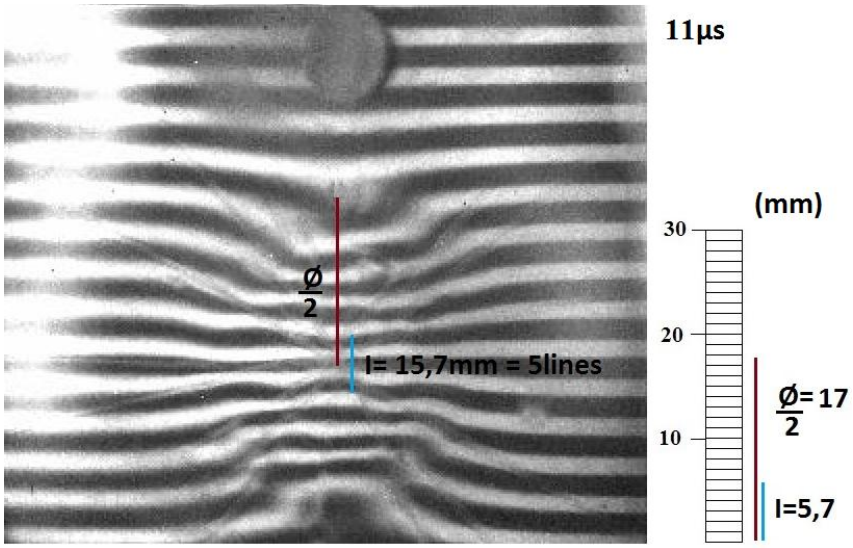

Figure 43- Image of a SiC tile during ballistic impact by a 7.62 APM2 bullet using deflectometry method to measure the dent size x 11µs after the first deformation of the tile's rear surface

Table 16 shows the results analyses of Figure 43. The dent size is 2.8 mm at the time of 11 µs after the first deformation appears on the projected lines on the SiC tile during ballistic impact. The dent size, x, is of 2,8mm. A much larger value than the one obtained using this technique on Al_2O_3 tile.

Table 16- Dent calculation Excel sheet for a 8mm thick SiC tile during ballistic impact by a 7.62 APM2 bullet using deflectometry method

16-23-16 experiment				**time**	**11µs**
Image	I	5,70E-03	m	Output	
Object	o	1,00E-02	m	Input	
I/o	M	5,70E-01			
Number of lines of the virtual image	n	5			
Distance between lines on grid	g	2,00E-03	m		
Distance of the object	d_0	7,30E-02	m		
Virtual distance	d_I	4,16E-02	m		
Focal point	f	2,65E-02	m		
Radius	R	5,30E-02	m		
Dent diameter	Ø	3,40E-02	m		
Dent radius	Ø/2	1,70E-02	m		
Dent size (optical)	x	2,80E-03	m	**2,8**	**x(mm)**

Figure 44 shows the relation between the dent size, x, and the time from 1 to 13µs. Two different patterns are visible, one from 3 to 7µs, and another from 9 to 13µs where the

dent increment is almost linear. Between 7 and 9μs there is a variation of the dent size increment that shows not to be linear. Once again, it is necessary to analyze the deformation velocity to understand this behavior.

Figure 45 shows the relation between the deformation velocity and time for 6 different times from 3 μs to 13 μs distanced by 2μs. It is visible by this graphic, the increment of velocity from 3 to 7μs, followed by a decrement from 7 to 9μs and finally an increment from 9 to 13μs. Once again, it is considered that this variation is due to the shock wave in the SiC tile provoked by the ballistic impact. It is interesting to see this behavior present in both experiments with different tile materials.

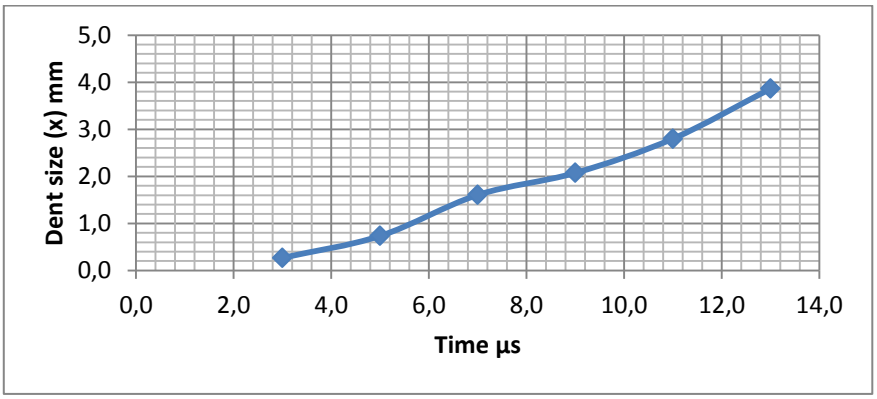

Figure 44- Relation between dent size (x) and time after impact of a SiC tile during ballistic impact by a 7.62 APM2 bullet

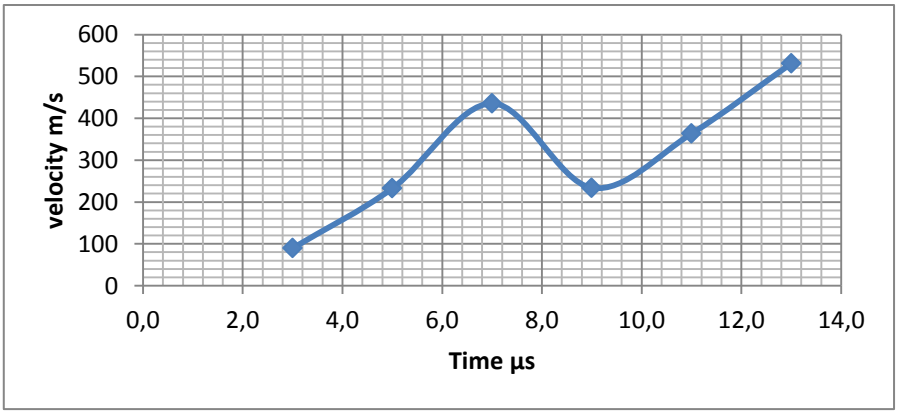

Figure 45- Relation between time after impact and the deformation velocity of a SiC tile during ballistic impact by a 7.62 APM2 bullet

Table 17 is the consolidation of the results obtained by Figure 44 and 45. The dent size, x, increases with a constant velocity during the first 7μs. After this moment it

suffers a decrement of the deformation velocity visible on the 9μs frame, increasing once again constantly from that moment forward.

Table 17- Dent size (x) and deformation velocity for 3 to 13μs during ballistic impact by a 7.62 APM2 bullet

x(mm)	v(m/s)	time (μs)
0,27	90	3
0,73	233	5
1,61	436	7
2,07	234	9
2,80	363	11
3,86	531	13

The experiment was repeated six times using the same ceramic tile and bullet velocity. Only one more of these six experiments allowed the Deflectometry technique to be used, due to the fact of only one more experiment had image data clear enough to give successful results. The reason of this default on various of the samples, is due to the camera settings such as trigger time or the compressed air gun accuracy Figure 46 shows the sequence of images from 1 to 11μs. The sequence of images has 4μs less than the last experiment with the same SiC material due to the shred of the polymer cover.

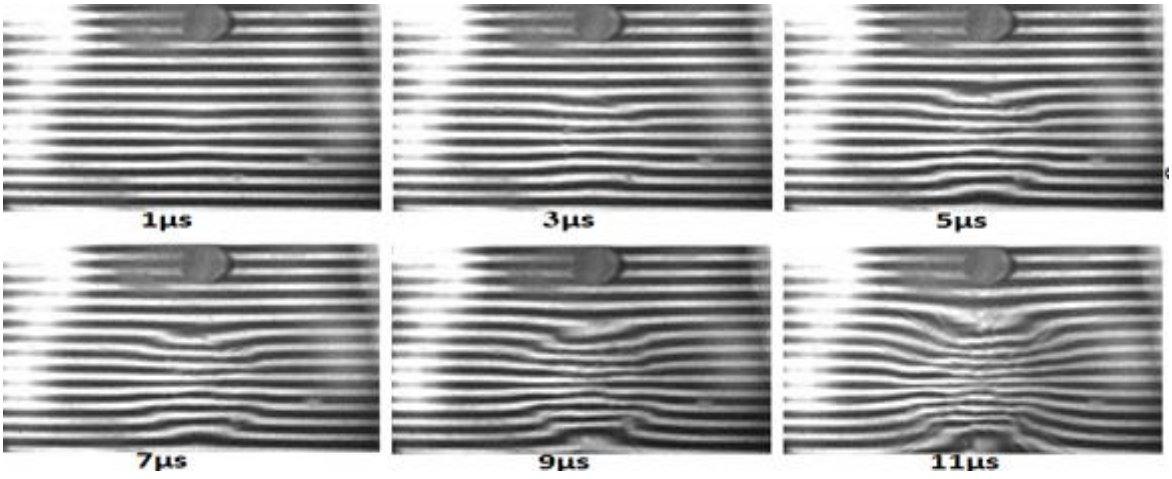

Figure 46-Different frames from projected lines on an SiC tile during ballistic impact by a 7.62 APM2 bullet

Figure 47 shows the relation between the dent size, x, and the frame time of the images after impact. With these results, we can make a relation between the previous experiment where the same parameters where utilized.

From 3 to 7µs, there is a near linear dent size increment, followed by a smaller dent development from 7 to 9µs and finally another increment from 9 to 11µs. In comparison with the last experiment, all variation behaviors were identical (Figure 44). The moments of variation of the dent development are the same, although the values of the dent size are not (maximum dent size on the first experiment was of 3.86mm and this experiment of 2.95mm). This can be due to the impact zone of the projectile on both SiC tiles being different.

Figure 48 show the results of the velocity of deformation on the SiC tile. We can verify a slight change in the deformation velocity in relation with the values of the last experiment (Figure 45). The shock wave occurs between 6 and 11µs that is when the dent size achieves the value of 2.14mm, a similar moment as the previous experiment with the value of 2.07mm (Figure 44).

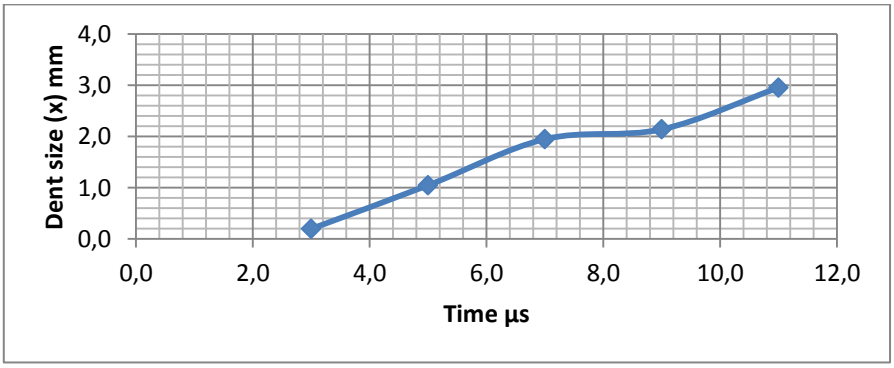

Figure 47- Relation between dent size (x) and time after impact of a SiC tile during ballistic impact by a 7.62 APM2 bullet

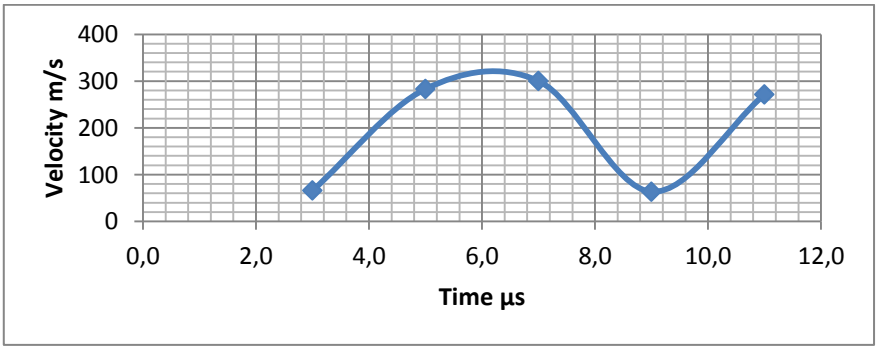

Figure 48- Relation between time after impact and the deformation velocity of a SiC tile during ballistic impact by a 7.62 APM2 bullet

Table 18 was once again elaborated to facilitate the comprehension of Figures 47 and 48. It is perceptible to see the different dent size values during 11µs moments after ballistic impact. The maximum value possible of obtaining with Deflectometry technique is of 2.95mm at 11µs.

Table 18- Dent size (x) and deformation velocity for 3 to 11µs during ballistic impact by a 7.62 APM2 bullet

x(mm)	v(m/s)	time (µs)
0,20	66	3
1,05	283	5
1,95	300	7
2,14	64	9
2,95	272	11

When the experimental results with previous studies (Carton E. P. and Roibrocks R, 2012), are compared, we can find a pattern in results for the transition between the maximum times possible to analyse using deflectometry (measuring at 13µs for 7mm Al_2O_3 tiles) and the minimum values obtain optically by previous studies (Carton E. P. and Roibrocks R, 2012), starting from 14µs for the same tile thickness. This gives support to the success of the use of deflectometry for measurement of ceramic tile deflection during ballistic impact.

5. CONCLUSIONS

This master thesis provides an overview of measuring techniques for the study of deflection on ceramic tiles during ballistic impact. There are three different matters that should be reflected on the conclusions of this work; they are:

- Measuring technique selected:
  a. Deflectometry measuring technique is simple, low cost and accurate method. Therefore, it was selected to determine the deflection of a ceramic tile during ballistic impact.

- Static Experiments:
  a. Static experiments are necessary to avoid unpleasant surprises during dynamic experiments;
  b. It is necessary to create a polymer coating in order to achieve reflective properties on ceramic tiles, necessary for the Deflectometry measuring technique;
  c. This technique is only possible when in presence of a perfectly spherical shaped dent;
  d. The position of the camera and grid is fundamental in a matter of obtain the smallest angle between them as possible and therefor have accurate results.

- Dynamic Experiments:
  a. Al_2O_3 material results:
     I. There are two linear deformation velocities between 3 and 7μs and also between 9 and 13μs;
     II. A shock wave is visible between 7 and 9μs.
     III. The first radial cracks appear at 7μs after impact;
     IV. The Deflectometry measuring technique is only possible for the first 13μs. After this moment, the polymer coating is destroyed.

b. SiC material results:
   I. Two Sic tiles were tested with deflectometry measuring technique obtaining similar results;
   II. There are two linear deformation velocities between 3 and 7μs and also between 9 and 11μs;
   III. A shock wave is visible between 7 and 11μs;
   IV. The first radial cracks appear 5μs after impact.

REFERENCES

Adams.B, (2003) Master thesis "Simulation of ballistic impacts on armored civil vehicles", Eindhoven University of Technology, pp. 6-10

Antonelli K., et al. (1999), "The measurement, Instrumentation and sensors Handbook", by CRC Press LLC, pp. 40,41.

Arbor Scientific., (2009) "Newton's Ring Apparatus", pp. 1-2.

Beynet P. and Plunkett R., (1971), "Plate Impact and Plastic Deformation by Projectiles", Investigation study,

Bornet M., et al, (2008) "Assessment of digital image correlation measurement errors: methodology and results", French CNRS research network 2519, pp. 4-6

Carton E.P., (2012), TNO report/ TNO-DV IN033.

Catalogue "Capacitive Position Sensors – Nanometrology Solutions" (2007), Physik Instrumente (PI), , pp. 4-5.

Creath K. and Wyant J. C., (1992) "Moiré and Fringe Projection Techniques", Optical shop testing, second edition.

Devivier C., et al., (2013) "Impact damage detection in composite plates using Deflectometry and virtual fields method", Composites: Part A 48 pp. 201–218.

Ditzhuijzen C.S.E., (January 2013), "High-speed X-ray eigenschappen'', Vertrouwelijk memorandum.

Ditzhuijzen C.S.E., (October 2013), Classified memorandum "Dynamic model of the bending of ceramic tiles during ballistic impact".

Ditzhuijzen C.S.E., et al., (August 2013), TNO report, "Real-time crack shadowgraphy of ceramic tiles during ballistic impact",

Feynman R., (1963), "The Feynman Lectures on Physics", Complete Volume 1, pp. 251-256.

Field J. E., et al., (2004) "Experimental techniques for high rate deformation and shock studies", International Journal of Impact Engineering 30, 725-775.

Frade J. F. C., (2012) Trainee Report, TNO.

Hammond R., (2004), Dissertation for the degree of Doctor of Philosophy, "Shock and ballistic properties of bainitic steels and tungsten alloys", pp.30-74

Lai Y., (2005) "Eddy Current Displacement Sensor with LTCC Technology", Dissertation zur Erlangung des Doktorgrades, pp.6-19

Lion Precision, (2013) "Eddy-Current Sensors", St. Paul, Mn USA, product Catalogue, pp.2-9

Mook G., et al., (2006), "Deep Penetrating Eddy Currents and Probes",.

Nagata T. et al. (2013) "The effects of a convex rear-view mirror on ocular

accommodative responses" Applied Ergonomics, pp.1039-1043.

Pretice H. J., et al., (2011) "Optical techniques for investigation of the ballistic impact of thin plates", International Journal of impact Engineering 38, pp. 849-863

Proulx T., (2013), "Application of imaging techniques to mechanics of materials and structures", volume 4, proceedings of the 2010 annual conference on experimental and applied mechanics, Springer, pp.217-224

Shepherd R. and Wensley L. M, (1965), "The Moiré-fringe method of displacement Measurement applied to indirect Structural-model analysis", Experimental Mechanics,

Surrel Y., (2009), "Deflectometry: a simple and efficient noninterferometric method for slope measurement", ENSAM Journal, pp.2-5

Umesh K. S., et al., (2012), "Revisiting Fizeau's Observations: Spectral study of NA source using Newton's rings", CISE 2011-12 Project pp. 2-3.

WEBSITES

[R1]- http://en.wikipedia.org/wiki/Capacitance

[R2]- http://www.lionprecision.com/capacitive-sensors/cap-products.html

[R3]- http://hyperphysics.phy-astr.gsu.edu/hbase/electric/farlaw.html